Multiuser Detection for Cooperative Networks and Performance Analysis

Luca Venturino, *Member, IEEE*, Xiaodong Wang, *Senior Member, IEEE*, and Marco Lops, *Senior Member, IEEE*

***Abstract*—We investigate strategies for user cooperation in the uplink of a synchronous direct-sequence code-division multiple-access (DS/CDMA) network employing nonorthogonal spreading codes and analyze their performance. We consider two repetition-based relay schemes: decode-and-forward (DAF) and amplify-and-forward (AAF). Focusing on the use of linear multiuser detectors, we first present cooperation strategies, i.e., signal processing at both the relay nodes and the base station (BS), under the assumption of perfectly known channel conditions of all links; then, we consider the more practical scenario where relays and BS have only partial information about the system parameters, which requires blind multiuser detection methods. We provide performance analysis of the proposed detection strategies in terms of the (asymptotic) signal-to-(interference plus noise) ratio and the bit error rate, and we show that AAF achieves a full second-order diversity when a minimum mean-square-error detector is employed at both the relay side and the BS. A simple, yet effective, partner selection algorithm is also presented. Finally, a thorough performance assessment is undertaken to study the impact of the multiple-access interference on the proposed cooperative strategies under different scenarios and system assumptions.**

***Index Terms*—Blind multiuser detection, cooperative diversity, direct-sequence code-division multiple-access (DS/CDMA), linear minimum mean-square-error detector (MMSE) detector.**

I. Introduction

COMMUNICATIONS over wireless channels suffer from fading induced by multipath propagation, which causes a random fluctuation in the received signal level. The effects of fading can be mitigated by transmitting and processing independent copies of the same signal. Well-known forms of diversity are spatial diversity, temporal diversity, and frequency diversity [1]. Spatial diversity is very attractive since it can be combined with other forms of diversity, while being the only alternative when time and frequency diversities are not available. A popular way of exploiting spatial diversity is to employ multiple colocated antennas at the transmitter and/or at the receiver. By using suitably designed space-time codes, a diversity gain and/or a multiplexing gain can be achieved at no cost in terms of transmission time and bandwidth expansion [2]–[4]. Unfortunately, due to size, cost, and hardware limitations, a wireless device may not always be able to support multiple transmit antennas. This is the case for most handsets in current cellular networks or for the nodes of wireless sensor networks. To overcome this limitation, a new form of space diversity, known as *user cooperation diversity,* has been recently proposed [5], [6]. This new technique takes advantage of the broadcast nature of the radio channel allowing (single-antenna) terminals in a multiuser environment to share their physical resources in order to create a virtual transmit and/or receive array through distributed transmission and signal processing [7]–[9]. More specifically, a cooperative transmission system consists of a set of wireless devices, which agree to relay messages for each other in order to propagate redundant copies of the same signal through independent paths to the final destination. Preliminary works [5], [6], [10] on user cooperation have mostly focused on the simplest case of two-user cooperation through orthogonal subchannels. Two basic cooperative strategies—decode-and-forward (DAF) and amplify-and-forward (AAF)—have been proposed and analyzed. Adaptive and incremental versions of these protocols have been investigated in [10], whereas in [11], the extension to an arbitrary group of cooperative users is considered. The use of distributed space-time coding has instead been proposed in [11]–[14].

Even though these initial works have already posed important milestones [15], showing the substantial potential benefits of user cooperation, much research still has to be done in order to gain insight into this promising technology. Several important issues need to be addressed, such as the impact of the multiple-access interference (MAI) [inevitably present in current nonorthogonal code-division multiple-access (CDMA) communication systems [16]] on the proposed cooperative protocols [17]; the choice of partner allocation strategy and its impact on the overall system performance; and the impact of imperfect knowledge of some system parameters on the correct combining of the direct and relayed signal replicas.

In this paper, we investigate these issues. In particular, we analyze the performance of user cooperation in the uplink of a synchronous direct-sequence (DS) CDMA cellular network employing nonorthogonal spreading codes. For the sake of simplicity, we assume that each cooperating terminal has only one partner to be used as relay [5], [10]. The contribution of this paper is manifold and can be summarized as follows.

- We consider two repetition-based relay strategies which generalize the cooperative protocols proposed in [5] and [10]—DAF and AAF—to a scenario where user cooperation takes place through nonorthogonal subchannels. Focusing on the use of the linear MMSE detector [18], we analyze the impact of the multiple access interference on

Manuscript received December 20, 2004; revised September 23, 2005. The associate editor coordinating the review of this manuscript and approving it for publication was Dr. Martin Haardt. The work of X. Wang was supported in part by the U.S. National Science Foundation (NSF) under grant CMS-0427353, and in part by the U.S. Office of Naval Research (ONR) under grant N00014-03-1-0039.

L. Venturino and M. Lops are with the DAEIMI Department, Università degli Studi di Cassino, 43 03043 Cassino (FR), Italy (e-mail: l.venturino@unicas.it; lops@unicas.it).

X. Wang is with the Electrical Engineering Department, Columbia University, New York, NY 10027 USA (e-mail: wangx@ee.columbia.edu).

Digital Object Identifier 10.1109/TSP.2006.877646

these protocols. We also investigate the effect of adopting a simple matched filter (MF) receiver at the relay terminals.

- The performance of cooperation is first studied under ideal system assumptions. Assuming that the residual interference is Gaussian distributed, conditioned on the fading channels, we provide closed-form expressions for the signal-to-(interference plus noise) ratio (SINR) and the bit error rate (BER); also, we show that AAF always achieves a full second-order diversity when an MMSE detector is employed at both the relay side and the BS, extending previous results of [9] and [10].
- The performance of cooperation is then investigated under more reasonable system assumptions. We assume that each relay has knowledge of only the channel and the spreading code of the terminal of interest, but not of those of the other interfering users, whereas the BS has knowledge of the spreading codes and the uplink channels of the active users only. In this scenario, blind multiuser detectors are employed [19]–[22]. At the relay side, we show that the exact MMSE detector can be blindly implemented once a sample estimate of the covariance matrix of the received signal is available. At the BS, instead, robust blind estimates of the MMSE detector cannot be derived without the feedback of some parameters related to the interpartner links. Closed-form expressions to approximate the asymptotic SINR and BER of these blind detectors are provided.
- Finally, we address the problem of how the partners should be assigned and managed in the network, and we present a simple, yet effective, partner selection strategy.

Using the analysis developed in this paper, the performance of DAF and AAF are investigated and compared under different scenarios. Simulation results indicate that, when an MMSE detector is employed at both the relay side and the BS, both protocols provide a significant performance gain with respect to the direct transmission, extending previous results of [5]–[10] and [17]. In this case, we show that the proposed partner allocation strategy may be effectively used to optimize the overall system performance, at least in stationary scenarios. Interestingly enough, even if inferior to AAF under ideal system assumptions, the DAF protocol turns out to be more amenable to blind multiuser detection when some system parameters are unknown.

The rest of this paper is organized as follows. In Section II, the network model and the cooperative protocols are described. In Section III, the relay strategies are presented and analyzed under ideal system assumptions. In Section IV, cooperation strategies under the assumption that some of the system parameters are unknown are proposed and analyzed. In Section V, a possible partner allocation strategy is discussed. In Section VI, some simulation results are presented. Section VII contains the conclusions. Finally, Appendix I contains some analytical derivations.

II. System Description

We consider a K-user synchronous DS/CDMA communication system employing nonorthogonal spreading codes, with processing gain N. We indicate with $k = 0$ the base station (BS) and with $k = 1, \ldots, K$ the active nodes. Without loss of generality, we assume that each terminal is able to simultaneously transmit and receive and that perfect echo cancellation is possible [5], [6]. To isolate the effects of user cooperation, we assume that all channels are frequency nonselective and that each mobile as well as the BS is equipped with only one antenna. Let $d_{k,q}$ be the distance between terminals k and q. We model the corresponding fading coefficient $\alpha_{k,q}$ as a circularly symmetric complex Gaussian random variable with variance $(1/d_{k,q})^a$, where a is the path-loss exponent. All channels remain constant during $2L$ consecutive symbol intervals, and $\alpha_{k,q} = \alpha_{q,k}$ due to the reciprocity of the channel. We point out that what follows could also be extended to the more general scenario of multiantenna terminals operating over dispersive channels. Indeed, user cooperation can also be used on top of other forms of diversity [10], [13].

Let $\mathcal{F} = \{1, 2, \ldots, P\}$, with $2 \leq P \leq K$, be the subset of cooperating terminals which decide to share their resources (namely, power and bandwidth). We assume that each user $k \in \mathcal{F}$ has a partner $f(k) \in \mathcal{F} \setminus \{k\}$, which is used as relay [5], [10]. Partnering is not necessarily bidirectional, in the sense that, if $P = 3$, it can happen that 1 relays for 2, 2 relays for 3, and, finally, 3 relays for 1 (see also [15]); the only important feature is that each cooperating user has a partner that provides a second data path, while being itself an active relay for another terminal. The issues of choosing the subset $\mathcal{F}$ of nodes that can effectively benefit from cooperation, and of defining the optimum mapping $f(\cdot)$, are open problems and, of course, may strongly influence the overall system performance. A possible solution is presented in Section V. Following [5] and [10], we assume that cooperation takes place in two phases as described below.

1) During the odd symbol intervals, each cooperating user transmits its own information (using its own spreading code), which is received by the BS as well as by the partner. In this phase, each cooperating terminal $f(k) \in \mathcal{F}$ attempts to recover from the received CDMA multiplex the data stream of the user $k \in \mathcal{F}$.
2) During the even symbol intervals, each partner relays a processed version of the information received in the previous symbol interval using its own spreading code. We discuss two relay strategies: a DAF strategy where the partners decode and retransmit the data stream of the user interest [5], [6], [10] and an AAF strategy where the partners simply amplify and forward soft estimates of the symbols of interest [10].

Indicating with $\{b_k(i), i = 1, \ldots, L\}, k \in \mathcal{F}$, the normalized symbol stream to be transmitted by each cooperating user and with $\{x_k(i), i = 1, \ldots, 2L\}, k \notin \mathcal{F}$, the symbol stream of the remaining noncooperative terminals, the discrete-time signals received at terminal $p = 0, 1, \ldots, P$ during the odd symbol intervals and at the BS during the even symbol intervals are given, respectively, by [16], [18], [19]

$$\boldsymbol{r}_p(2i-1) = \sum_{k=1, k\neq p}^{P} \sqrt{(2-\rho_k)}\boldsymbol{s}_{k,p} b_k(i) + \sum_{k=P+1}^{K} \boldsymbol{s}_{k,p} x_k(2i-1) + \boldsymbol{n}_p(2i-1) \quad (1)$$

$$\boldsymbol{r}_0(2i) = \sum_{k=1}^{P} \sqrt{\rho_{f(k)}}\boldsymbol{s}_{f(k),0}\tilde{b}_k(i) + \sum_{k=P+1}^{K} \boldsymbol{s}_{k,0}x_k(2i) + \boldsymbol{n}_0(2i), \quad i = 1,\ldots,L \quad (2)$$

where $\boldsymbol{s}_{k,p} = \sqrt{\mathcal{E}_k}\alpha_{k,p}\boldsymbol{c}_k$ is the filtered signature of the kth user received at terminal p, $\mathcal{E}_k$ and $\boldsymbol{c}_k$ is the symbol energy and the N-dimensional unit-energy signature vector, respectively; $\tilde{b}_k(i)$ represents either a hard or a soft estimate of $b_k(i)$, depending on whether a DAF or an AAF protocol is adopted: in the latter case, we assume that $\tilde{b}_k(i)$ is normalized to have unit variance. $\boldsymbol{n}_p(2i-1)$ and $\boldsymbol{n}_0(2i)$ are N-dimensional, circularly symmetric, white Gaussian noise vectors received at terminal p during the first phase and at the BS during the second phase, respectively; we assume that $\mathrm{E}[\boldsymbol{n}_p(2i-1)\boldsymbol{n}_0(2i)^H] = \boldsymbol{O}_N$ for $p = 0,\ldots,P$, $\mathrm{E}[\boldsymbol{n}_p(2i-1)\boldsymbol{n}_n(2i-1)^H] = \delta_{p,n}\mathcal{N}_p\boldsymbol{I}_N$ and $\mathrm{E}[\boldsymbol{n}_0(2i)\boldsymbol{n}_0(2i)^H] = \mathcal{N}_0\boldsymbol{I}_N$, where $\boldsymbol{O}_N$ is an $N \times N$ all-zero matrix and $\boldsymbol{I}_N$ is the $N \times N$ identity matrix (notice that the noise power at terminals $p = 0,\ldots,P$ may be different). Finally, $\rho_k \in [0,2]$ is a weighing factor that controls the power allocation of each cooperating user during the two phases of the protocol [5], [6], [15]. Notice that no extra power is injected into the system when a node decides to switch from a noncooperative to a cooperative mode (indeed, in both cases, an average energy $2\mathcal{E}_k$ is transmitted over two consecutive symbol intervals); thus, the totally consumed average power in the network is independent of the number of cooperating mobiles. Determining the optimum power allocation scheme for the cooperating terminals is beyond the scope of this paper; for the sake of simplicity, in the sequel we suboptimally assume that the available power is equally split during the two phases of the protocol, i.e., $\rho_k = 1$ for $k = 1,\ldots,P$.

Even though each user maintains the same average power constraint, the repetition nature of the cooperative protocols wastes half the available bandwidth [5], [10], [11]. Thus, to make a fair comparison between the transmission schemes with or without cooperation, the spectral efficiency of each user should be doubled when it switches from a noncooperative to a cooperative mode. In the sequel, unless otherwise stated, we consider an uncoded system where all users employ a quadrature phase-shift keying (QPSK) signaling, i.e., $b_k(i), x_k(i) \in \{\pm(1+j)/\sqrt{2}, \pm(1-j)/\sqrt{2}\}$, and we assume that the noncooperating users retransmit each QPSK symbol twice, i.e., $x_k(2i-1) = x_k(2i)$ for $i = 1,\ldots,L$: in this setup, all users send two new bits every two symbol intervals. This choice is suggested by the fact that repetition-based cooperative protocols are effective only in the low-spectral efficiency regime [10]. For higher spectral efficiencies, incremental or distributed space-time encoded cooperative protocols should be better employed [10]–[14]. Nevertheless, we remark that our results also apply to larger M-PSK constellations, as will be pointed out in the sequel.

III. Relay Strategies and Performance Analysis Under Ideal System Assumptions

In this section, we propose and analyze cooperative strategies for nonorthogonal CDMA networks under the assumption that all system parameters (namely, the interusers channels, the uplink channels, the spreading codes, and the relayed noise power) are perfectly known at the BS as well as at each cooperating terminal. Previous works on user cooperation have assumed that terminals cooperate on orthogonal subchannels, which simplifies the relay problem and the corresponding analysis. For example, in [9]–[14], a time-division (or a frequency-division) multiple-access transmission format is considered and, thus, the symbols of interest are easily recovered by using a time-windowing (passband) filter tuned to the desired time (frequency) slot. In [5] and [6], instead, a CDMA network with orthogonal spreading codes is considered: in this case, a simple MF detector is sufficient to extract the data stream of the user of interest from the received multiplex. On the other hand, when a nonorthogonal CDMA is employed, an MF receiver is no longer optimum, but better receive strategies may be adopted for MAI mitigation [16]. Focusing on the use of linear multiuser detection strategies, we propose to employ an MMSE detector at both the relays and the BS. For the sake of comparison, we also study the effect of using a reduced-complexity single-user receiver at the relay side.

In the sequel, we first focus on the relay operation performed at each cooperating terminal during the odd symbol intervals; then, we address the problem of optimally combining the signals received at the BS.

A. Relay Strategies

Let $f(q) \in \mathcal{F}$ be the terminal of interest. We need to estimate the symbol $b_q(i)$ transmitted by user q during the odd symbol intervals, for $q = 1,\ldots,P$. The corresponding MF receiver is given by $\boldsymbol{m}_{q,f(q)} = \boldsymbol{s}_{q,f(q)}$, while the MMSE detector can be constructed as[1] [16], [18]

$$\boldsymbol{m}_{q,f(q)} = \boldsymbol{C}_{f(q)}^{-1}\boldsymbol{s}_{q,f(q)}$$
$$\text{with} \quad \boldsymbol{C}_{f(q)} \triangleq \mathrm{E}\left[\boldsymbol{r}_{f(q)}(2i-1)\boldsymbol{r}_{f(q)}(2i-1)^H\right] = \sum_{k=1,k\neq f(q)}^{K} \boldsymbol{s}_{k,f(q)}\boldsymbol{s}_{k,f(q)}^H + \mathcal{N}_{f(q)}\boldsymbol{I}_N. \quad (3)$$

Let $\xi \triangleq \boldsymbol{m}_{q,f(q)}^H\boldsymbol{r}_{f(q)}(2i-1)$ be the output of $\boldsymbol{m}_{q,f(q)}$ (either MF or MMSE); we distinguish two relay strategies.

1) DAF: As in [5] and [6], we assume that each partner fully decodes and retransmits the symbols of interest received during the first phase of the protocol. For this reason, we refer to this strategy as decode-and-forward. Let

$$\tilde{b}_q(i) = (\mathrm{sgn}[\Re\{\xi\}] + j\,\mathrm{sgn}[\Im\{\xi\}])/\sqrt{2}, \quad i = 1,\ldots,L \quad (4)$$

be the decoded symbols to be relayed. Given the fading channel states[2] $\boldsymbol{\alpha}_m = [\alpha_{1,m},\ldots,\alpha_{K,m}]$ and assuming that the residual MAI is Gaussian distributed, the conditional BER can be expressed as [18]

$$\mathrm{P}_{q,f(q)}\left(\boldsymbol{\alpha}_{f(q)}\right) = Q\left(\sqrt{\mathrm{SINR}_{q,f(q)}\left(\boldsymbol{\alpha}_{f(q)}\right)}\right) \quad (5)$$

[1]From now on, unless otherwise stated, all expectations are conditioned upon the channel state.

[2]For notational simplicity, we define $\alpha_{m,m} = 0$.

where $Q(x) = (1/\sqrt{2\pi})\int_x^{+\infty} e^{-(t^2/2)}\,dt$ and $\mathrm{SINR}_{q,f(q)}(\boldsymbol{\alpha}_{f(q)})$ is the conditional output SINR given by

$$\begin{aligned}\mathrm{SINR}_{q,f(q)}&\left(\boldsymbol{\alpha}_{f(q)}\right)\\ &= \frac{\mathrm{E}[\Re\{\xi\}\,|\,\Re\{b_q(i)\}]^2}{\mathrm{Var}[\Re\{\xi\}\,|\,\Re\{b_q(i)\}]} = \frac{\mathrm{E}[\Im\{\xi\}\,|\,\Im\{b_q(i)\}]^2}{\mathrm{Var}[\Im\{\xi\}\,|\,\Im\{b_q(i)\}]}\\ &= \frac{\frac{1}{2}\Re\left\{\boldsymbol{m}_{q,f(q)}^H\boldsymbol{s}_{q,f(q)}\right\}^2}{\frac{1}{2}\sum_{\substack{k=1\\k\neq q,f(q)}}^{K}\left|\boldsymbol{m}_{q,f(q)}^H\boldsymbol{s}_{k,f(q)}\right|^2+\frac{\mathcal{N}_{f(q)}}{2}\|\boldsymbol{m}_{q,f(q)}\|^2}.\end{aligned} \tag{6}$$

The Gaussian assumption is very accurate for the MMSE detector as shown in [18] and [20], whereas for the MF receiver is sufficiently accurate at low signal-to-noise ratios (SNRs) and/or when the number of users approaches the processing gain [23].

2) AAF: Paralleling [10], we propose that each relay amplifies and forwards the signal at the output of the receive linear filter (either MF or MMSE). This strategy extends the original protocol of [10] to the case where user cooperation takes place through nonorthogonal subchannels and, for this reason, is referred to as amplify-and-forward. In this case, the following soft symbol estimate is forwarded to the BS:

$$\begin{aligned}\tilde{b}_q(i) = \frac{\boldsymbol{m}_{q,f(q)}^H\boldsymbol{r}_{f(q)}(2i-1)}{G_{f(q)}} &= \underbrace{\psi_{q,f(q)}b_q(i)}_{\text{Useful signal}}\\ &+\underbrace{\sum_{\substack{k=1\\k\neq q,f(q)}}^{P}\psi_{k,f(q)}b_k(i)+\sum_{k=P+1}^{K}\psi_{k,f(q)}x_k(2i-1)}_{\text{Residual Interference}}\\ &+\underbrace{v_{f(q)}(2i-1)}_{\text{Filtered Noise}}\end{aligned} \tag{7}$$

where

$$\begin{aligned}\psi_{k,f(q)} &\triangleq \frac{\boldsymbol{m}_{q,f(q)}^H\boldsymbol{s}_{k,f(q)}}{G_{f(q)}}\\ v_{f(q)}(2i-1) &\triangleq \frac{\boldsymbol{m}_{q,f(q)}^H\boldsymbol{n}_{f(q)}(2i-1)}{G_{f(q)}}\end{aligned} \tag{8}$$

while

$$\begin{aligned}G_{f(q)} &\triangleq \left(\mathrm{E}\left[\left|\boldsymbol{m}_{q,f(q)}^H\boldsymbol{r}_{f(q)}(2i-1)\right|^2\right]\right)^{\frac{1}{2}}\\ &= \left(\sum_{k=1,k\neq f(q)}^{K}\left|\boldsymbol{m}_{q,f(q)}^H\boldsymbol{s}_{k,f(q)}\right|^2\mathcal{N}_{f(q)}\left\|\boldsymbol{m}_{q,f(q)}\right\|^2\right)^{\frac{1}{2}}\end{aligned} \tag{9}$$

is just a power normalization factor ensuring that $\mathrm{E}[|\tilde{b}_q(i)|^2] = 1$ (i.e., that no extra power is injected into the system by the relay terminal).

From (7), it is seen that the relayed useful signal is corrupted by both noise and some residual MAI. When an MMSE receiver is employed, the residual MAI is asymptotically nullified at the price of possibly enhancing the received noise: in this case, each partner substantially relays only the symbol of interest plus noise as in [10]. On the other hand, when an MF is employed, the received noise is not enhanced, but an MAI leakage is present. In this case, each partner also amplifies and forwards unwanted signals coming from interfering users that are not taking part in the cooperation process. In Section VI, we will study the effect of having these unwanted relayed signals.

B. Performance Analysis of DAF

When each partner forwards a hard estimate of the symbol of interest, upon defining

$$\begin{aligned}&\boldsymbol{r}(i) \triangleq \begin{bmatrix}\boldsymbol{r}_0(2i-1)\\ \boldsymbol{r}_0(2i)\end{bmatrix},\quad \boldsymbol{h}_k^{(1)} \triangleq \begin{bmatrix}\boldsymbol{s}_{k,0}\\ \boldsymbol{0}_N\end{bmatrix},\\ &\boldsymbol{h}_k^{(2)} \triangleq \begin{bmatrix}\boldsymbol{0}_N\\ \boldsymbol{s}_{k,0}\end{bmatrix},\quad \boldsymbol{h}_k \triangleq \begin{bmatrix}\boldsymbol{s}_{k,0},\\ \boldsymbol{s}_{k,0}\end{bmatrix},\\ &\boldsymbol{n}(i) \triangleq \begin{bmatrix}\boldsymbol{n}_0(2i-1)\\ \boldsymbol{n}_0(2i)\end{bmatrix}\end{aligned} \tag{10}$$

with $\boldsymbol{0}_N$ an N-dimensional all-zero vector, the signals (1) and (2) received at the BS during the odd and even symbol intervals, respectively, can be stacked as follows:

$$\boldsymbol{r}(i) = \sum_{k=1}^{P}\boldsymbol{H}_k\boldsymbol{b}_k(i)+\sum_{k=P+1}^{K}\boldsymbol{h}_k x_k(2i)+\boldsymbol{n}(i) \tag{11}$$

where $\boldsymbol{H}_k \triangleq [\boldsymbol{h}_k^{(1)}, \boldsymbol{h}_{f(k)}^{(2)}], \boldsymbol{b}_k(i) \triangleq [b_k(i), \tilde{b}_k(i)]^T, \tilde{b}_k(i)$ is given by (4) and we have exploited the fact that $x_k(2i-1) = x_k(2i)$. The linear MMSE detector for a user $q \in \mathcal{F}$ is given by

$$\boldsymbol{m}_q = \mathrm{E}[\boldsymbol{r}(i)\boldsymbol{r}(i)^H]^{-1}\mathrm{E}[\boldsymbol{r}(i)b_q(i)^*] = \boldsymbol{C}_r^{-1}\bar{\boldsymbol{h}}_q \tag{12}$$

with

$$\begin{aligned}\bar{\boldsymbol{h}}_q &\triangleq \mathrm{E}[\boldsymbol{r}(i)b_q(i)^*]\\ &= \boldsymbol{h}_q^{(1)}+\left[1-2P_{q,f(q)}\left(\boldsymbol{\alpha}_{f(q)}\right)\right]\boldsymbol{h}_{f(q)}^{(2)}\end{aligned} \tag{13}$$

$$\begin{aligned}\boldsymbol{C}_r &\triangleq \mathrm{E}[\boldsymbol{r}(i)\boldsymbol{r}(i)^H] = \sum_{k=1}^{P}\boldsymbol{H}_k\boldsymbol{B}_k\boldsymbol{H}_k^H\\ &\quad+\sum_{k=P+1}^{K}\boldsymbol{h}_k\boldsymbol{h}_k^H+\mathcal{N}_0\boldsymbol{I}_{2N}\end{aligned} \tag{14}$$

$$\begin{aligned}\boldsymbol{B}_k &\triangleq \mathrm{E}[\boldsymbol{b}_k(i)\boldsymbol{b}_k(i)^H]\\ &= \begin{bmatrix}1 & 1-2P_{k,f(k)}\left(\boldsymbol{\alpha}_{f(k)}\right)\\ 1-2P_{k,f(k)}\left(\boldsymbol{\alpha}_{f(k)}\right) & 1\end{bmatrix}.\end{aligned} \tag{15}$$

In (13)–(15), we have used the fact that $\mathrm{E}[b_q(i)\tilde{b}_q(i)^*] = 1 - 2P_{q,f(q)}(\boldsymbol{\alpha}_{f(q)})$, where $P_{q,f(q)}(\boldsymbol{\alpha}_{f(q)})$ is given by (5). The decision statistic is

$$\xi \triangleq \boldsymbol{m}_q^H \boldsymbol{r}(i) = \boldsymbol{m}_q^H \left[\boldsymbol{h}_q^{(1)} + \delta_q(i)\boldsymbol{h}_{f(q)}^{(2)}\right] b_q(i) + \underbrace{\sum_{k=1,k\neq q}^{P} \boldsymbol{m}_q^H \boldsymbol{H}_k \boldsymbol{b}_k(i) + \sum_{k=P+1}^{K} \boldsymbol{m}_q^H \boldsymbol{h}_k x_k(2i) + \boldsymbol{m}_q^H \boldsymbol{n}(i)}_{z_q(i)} \tag{16}$$

where $\delta_q(i)$ is a random variable specified as follows:

$$\begin{aligned} &\Pr\{\delta_q(i) = 1\} \\ &\quad = 1 - \left\{2P_{q,f(q)}\left(\boldsymbol{\alpha}_{f(q)}\right) - \left[P_{q,f(q)}\left(\boldsymbol{\alpha}_{f(q)}\right)\right]^2\right\} \\ &\Pr\{\delta_q(i) = -1\} \\ &\quad = \left[P_{q,f(q)}\left(\boldsymbol{\alpha}_{f(q)}\right)\right]^2 \\ &\Pr\{\delta_q(i) = \pm j\} \\ &\quad = P_{q,f(q)}\left(\boldsymbol{\alpha}_{f(q)}\right)\left[1 - P_{q,f(q)}\left(\boldsymbol{\alpha}_{f(q)}\right)\right]. \end{aligned} \tag{17}$$

A final decision on the symbol of interest is given by $\hat{b}_q(i) = (\mathrm{sgn}[\Re\{\xi\}] + j\mathrm{sgn}[\Im\{\xi\}])/\sqrt{2}$. Thus, assuming that the residual interference is Gaussian distributed, conditioned on the channel state $\boldsymbol{\alpha} = [\boldsymbol{\alpha}_0, \boldsymbol{\alpha}_1, \ldots, \boldsymbol{\alpha}_P]$, the corresponding BER can be expressed as

$$\mathrm{P}_q(\boldsymbol{\alpha}) = \sum_{\lambda\in\{\pm 1,\pm j\}} \Pr\{\delta_q(i) = \lambda\} Q\left(\sqrt{\mathrm{SINR}_q(\boldsymbol{\alpha},\lambda)}\right) \tag{18}$$

with

$$\begin{aligned} &\mathrm{SINR}_q(\boldsymbol{\alpha},\lambda) \\ &\quad = \frac{\mathrm{E}[\Re\{\xi\} \mid \Re\{b_q(i)\}, \delta_q(i) = \lambda]^2}{\mathrm{Var}[\Re\{\xi\} \mid \Re\{b_q(i)\}, \delta_q(i) = \lambda]} \\ &\quad = \frac{\frac{1}{2}\Re\left\{\boldsymbol{m}_q^H\left(\boldsymbol{h}_q^{(1)} + \lambda\boldsymbol{h}_{f(q)}^{(2)}\right)\right\}^2}{\frac{1}{2}\Im\left\{\boldsymbol{m}_q^H\left(\boldsymbol{h}_q^{(1)} + \lambda\boldsymbol{h}_{f(q)}^{(2)}\right)\right\}^2 + \phi + \|\boldsymbol{m}_q\|^2\frac{\mathcal{N}_0}{2}} \end{aligned} \tag{19}$$

$$\begin{aligned} \phi &\triangleq \mathrm{E}[\Re\{z_q(i)\}\Re\{z_q(i)\}] \\ &= \frac{1}{2}\sum_{k=1,k\neq q}^{P}\left[\left\|\boldsymbol{m}_q^H\boldsymbol{H}_k\right\|^2 + 2\left(1 - 2P_{k,f(k)}\left(\boldsymbol{\alpha}_{f(k)}\right)\right)\right. \\ &\quad \left.\times\,\Re\left\{\left(\boldsymbol{m}_q^H\boldsymbol{h}_k^{(1)}\right)\left(\boldsymbol{m}_q^H\boldsymbol{h}_{f(k)}^{(2)}\right)^*\right\}\right] \\ &\quad + \frac{1}{2}\sum_{k=P+1}^{K}\left|\boldsymbol{m}_q^H\boldsymbol{h}_k\right|^2. \end{aligned} \tag{20}$$

The unconditional BER can be evaluated by averaging (18) over $\boldsymbol{\alpha}$ using Monte Carlo techniques. Finally, notice that the above analysis can also be extended to evaluate the performance of the noncooperative users. However, for brevity, we omit the derivation.

C. Performance Analysis of AAF

When each partner forwards a soft estimate of the symbol of interest to the BS, substituting (7) in (2), we have

$$\begin{aligned} \boldsymbol{r}_0(2i) &= \sum_{k=1}^{P}\bar{\boldsymbol{s}}_{k,0}b_k(i) + \sum_{k=P+1}^{K}\bar{\boldsymbol{s}}_{k,0}x_k(2i-1) \\ &\quad + \sum_{k=P+1}^{K}\boldsymbol{s}_{k,0}x_k(2i) + \bar{\boldsymbol{n}}_0(2i) \end{aligned} \tag{21}$$

with

$$\begin{aligned} \bar{\boldsymbol{s}}_{k,0} &= \sum_{p=1,f(p)\neq k}^{P}\boldsymbol{s}_{f(p),0}\psi_{k,f(p)}, \quad k = 1,\ldots,K \\ \bar{\boldsymbol{n}}_0(2i) &= \sum_{k=1}^{P}\boldsymbol{s}_{f(k),0}v_{f(k)}(2i-1) + \boldsymbol{n}_0(2i). \end{aligned} \tag{22}$$

In (21) and (22), $\{\bar{\boldsymbol{s}}_{k,0}, k = 1,\ldots,K\}$ are the composite signatures received at the BS during the even symbol intervals, accounting for the MAI leakage present at the output of the receive linear filter employed at the relays (see (7)); $\bar{\boldsymbol{n}}_0(2i)$ is an equivalent noise vector accounting for both the current noise and the relayed noise. The signals (1) and (21) received at the BS during the odd and even symbol intervals, respectively, can now be stacked to obtain

$$\begin{aligned} \boldsymbol{r}(i) &= \sum_{k=1}^{P}\bar{\boldsymbol{h}}_k b_k(i) + \sum_{k=P+1}^{K}\bar{\boldsymbol{h}}_k x_k(2i-1) \\ &\quad + \sum_{k=P+1}^{K}\boldsymbol{h}_k^{(2)}x_k(2i) + \boldsymbol{n}(i) \end{aligned} \tag{23}$$

$$= \sum_{k=1}^{P}\bar{\boldsymbol{h}}_k b_k(i) + \sum_{k=P+1}^{K}\bar{\boldsymbol{u}}_k x_k(2i) + \bar{\boldsymbol{n}}(i) \tag{24}$$

where $\boldsymbol{r}(i)$ and $\boldsymbol{h}_k^{(2)}$ are defined in (10) and

$$\begin{aligned} \bar{\boldsymbol{h}}_k &\triangleq \begin{bmatrix}\boldsymbol{s}_{k,0}\\ \bar{\boldsymbol{s}}_{k,0}\end{bmatrix}, \quad \bar{\boldsymbol{u}}_k \triangleq \begin{bmatrix}\boldsymbol{s}_{k,0}\\ \bar{\boldsymbol{s}}_{k,0} + \boldsymbol{s}_{k,0}\end{bmatrix} = \bar{\boldsymbol{h}}_k + \boldsymbol{h}_k^{(2)} \\ \bar{\boldsymbol{n}}(i) &\triangleq \begin{bmatrix}\boldsymbol{n}_0(2i-1)\\ \bar{\boldsymbol{n}}_0(2i)\end{bmatrix} \end{aligned} \tag{25}$$

while in (24) we have exploited the fact that $x(2i-1) = x(2i)$. The linear MMSE detector for a user $q \in \mathcal{F}$ is $\boldsymbol{m}_q = \mathrm{E}[\boldsymbol{r}(i)\boldsymbol{r}(i)^H]^{-1}\mathrm{E}[\boldsymbol{r}(i)b_q(i)^*] = \boldsymbol{C}_r^{-1}\bar{\boldsymbol{h}}_q$, with $\bar{\boldsymbol{h}}_q$ given by (25) and

$$\begin{aligned} \boldsymbol{C}_r &\triangleq \mathrm{E}[\boldsymbol{r}(i)\boldsymbol{r}(i)^H] = \sum_{k=1}^{P}\bar{\boldsymbol{h}}_k\bar{\boldsymbol{h}}_k^H \\ &\quad + \sum_{k=P+1}^{K}\bar{\boldsymbol{u}}_k\bar{\boldsymbol{u}}_k^H + \boldsymbol{R}_{\bar{n}} \end{aligned} \tag{26}$$

$$\begin{aligned} \boldsymbol{R}_{\bar{n}} &\triangleq \mathrm{E}[\bar{\boldsymbol{n}}(i)\bar{\boldsymbol{n}}(i)^H] = \sum_{k=1}^{P}\boldsymbol{h}_{f(k)}^{(2)} \\ &\quad \times\left(\boldsymbol{h}_{f(k)}^{(2)}\right)^H\frac{\mathcal{N}_{f(k)}\left\|\boldsymbol{m}_{k,f(k)}\right\|^2}{G_{f(k)}^2} + \mathcal{N}_0\boldsymbol{I}_{2N}. \end{aligned} \tag{27}$$

Let $\xi \triangleq \boldsymbol{m}_q^H\boldsymbol{r}(i)$ be the decision statistic. A final decision on $b_q(i)$ is given by $\hat{b}_q(i) = (\mathrm{sgn}[\Re\{\xi\}] + j\mathrm{sgn}[\Im\{\xi\}])/\sqrt{2}$. Thus,

assuming that the residual MAI is Gaussian distributed, the conditional BER can be expressed as

$$\mathrm{P}_q(\boldsymbol{\alpha}) = Q\left(\sqrt{\mathrm{SINR}_q(\boldsymbol{\alpha})}\right) \tag{28}$$

with (29) as shown at the bottom of the page. As in the DAF case, the above analysis can be extended to evaluate the performance of the noncooperating users.

Averaging (28) over the fading channels is generally prohibitive and, thus, Monte Carlo techniques may be employed. However, when a linear MMSE detector is used at the relays, the following result provides an upper bound to the average BER of the proposed AAF protocol (see Appendix I for the derivation).

Proposition 1: Assume that a linear MMSE detector is employed at both the relay side and the BS. Under Rayleigh fading, at high SNRs, we have

$$\bar{\mathrm{P}}_q \triangleq \mathrm{E}_{\boldsymbol{\alpha}}\left[\mathrm{P}_q(\boldsymbol{\alpha})\right] \leq \frac{4}{\bar{\gamma}_{q,0}\bar{\gamma}_{q,f(q)}} + \frac{4}{\bar{\gamma}_{q,0}\bar{\gamma}_{f(q),0}} + \mathcal{O}\left(\frac{1}{\bar{\gamma}_{q,0}\bar{\gamma}_{f(q),0}}\right) + \mathcal{O}\left(\frac{1}{\bar{\gamma}_{q,0}\bar{\gamma}_{q,f(q)}}\right) \tag{30}$$

where $\mathrm{P}_q(\boldsymbol{\alpha})$ is given by (28), $\bar{\gamma}_{q,m} \triangleq \mathrm{E}[(\mathcal{E}_q|\alpha_{q,m}|^2)/(\sigma^2_{q,m})], \sigma^2_{q,m} = \mathcal{N}_q\|\mathcal{P}^{\perp}_{q,m}\|^2$, while

$$\mathcal{P}^{\perp}_{q,m} \triangleq \boldsymbol{C}_m\left(\boldsymbol{C}_m^H\boldsymbol{C}_m\right)^{\dagger}\boldsymbol{e}_q \qquad \boldsymbol{C}_m = [\boldsymbol{c}_1,\ldots,\boldsymbol{c}_{m-1},\boldsymbol{0}_N,\boldsymbol{c}_{m+1},\ldots,\boldsymbol{c}_K]. \tag{31}$$

In (31), $(\cdot)^{\dagger}$ indicates the Moore–Penrose pseudoinverse and $\boldsymbol{e}_q$ is the qth unit vector in $\mathbb{R}^K$.

Interestingly, the bound in (30) shows that, when linear multiuser detection is employed, AAF achieves a full second-order diversity from the direct and the relayed link, extending the results of [9] and [10].

Remark: The above analysis can also be extended to the case where the cooperating users employ a modulation format M-PSK, with $M > 4$. Focusing, for example, on the AAF protocol, the signal received during the two phases of the protocol can still be expressed as in (23). Notice that, if $\sqrt{M}$ is an integer, the noncooperating users may transmit either an M-PSK twice or two $\sqrt{M}$-PSK in two consecutive symbol intervals. It is, however, intuitive that this latter strategy is not inferior to the former. Indeed, neither one achieves any diversity gain, but using an $\sqrt{M}$-PSK constellation with average energy $\mathcal{E}$ ensures a larger minimum distance than using an M-PSK constellation with energy $2\mathcal{E}$ when $M > 4$ (being exactly equal for $M = 4$) [1], whereby, in the sequel, we assume that $\sqrt{M}$ is an integer and we use a $\sqrt{M}$-PSK constellation for the noncooperative users. Using the Gaussian approximation for the residual MAI and the analysis in [1], assuming Gray-mapping, the conditional BER can be well approximate at high SNRs by

$$\mathrm{P}_q(\boldsymbol{\alpha}) \simeq \frac{2}{\log_2 M} Q\left(\sqrt{2\cdot\mathrm{SINR}_q(\boldsymbol{\alpha})}\sin\left(\frac{\pi}{M}\right)\right) \tag{32}$$

with (33) as shown at the bottom of the page.

Similar developments apply to the DAF protocol. In this latter case, however, an exact closed-form characterization of the discrete random variable $\delta_q(i)$ in (16) may be difficult to derive, making the analysis more tedious.

IV. Relay Strategies and Performance Analysis Under Realistic System Assumptions

In this section, we propose and analyze cooperative protocols under more realistic system assumptions. We assume that each relay has knowledge of only the propagation channel and the spreading code of the terminal of interest, but not of those of the other interfering users. Indeed, while it may be reasonable to assume that the interpartner channel is periodically estimated (by using for example training symbols), it is unrealistic that each relay tracks the links of all others mobiles. Moreover, in practical cellular networks, the spreading code of the surrounding users may be unknown at each mobile terminal. On the other hand, we assume that the BS has knowledge of only the spreading codes and the uplink channels of all the active nodes. In the above scenario, the exact linear MMSE detectors derived in Section III cannot be evaluated either at the relays or at the BS. Using the recent literature on blind linear multiuser detection [19]–[22], we now show how robust estimates of these detectors can be derived and we analyze their performance.

A. Relay Strategies

Let the eigendecomposition of $\boldsymbol{C}_{f(q)}$ in (3) be $\boldsymbol{C}_{f(q)} = \boldsymbol{U}_s\boldsymbol{\Lambda}_s\boldsymbol{U}_s^H + \boldsymbol{U}_n\boldsymbol{\Lambda}_n\boldsymbol{U}_n^H$, where[3] $\boldsymbol{\Lambda}_s = \mathrm{Diag}(\lambda_1,\ldots,\lambda_{K-1})$ contains the largest $K-1$ eigenvalues of $\boldsymbol{C}_{f(q)}$; $\boldsymbol{U}_s = [\boldsymbol{u}_1,\ldots,\boldsymbol{u}_{K-1}]$ contains the eigenvectors corresponding to the largest $K-1$ eigenvalues in $\boldsymbol{\Lambda}_s$; $\boldsymbol{\Lambda}_n = \mathcal{N}_{f(q)}\boldsymbol{I}_{N-K+1}$; and $\boldsymbol{U}_n = [\boldsymbol{u}_K,\ldots,\boldsymbol{u}_N]$ contains the remaining eigenvectors corresponding to the smallest eigenvalue $\mathcal{N}_{f(q)}$. The linear

[3]Notice that for notational simplicity, the dependence of the eigencomponents on the receiving terminal $f(q)$ has been dropped.

$$\mathrm{SINR}_q(\boldsymbol{\alpha}) = \frac{\mathrm{E}[\Re\{\xi\}\,|\,\Re\{b_q(i)\}]^2}{\mathrm{Var}[\Re\{\xi\}\,|\,\Re\{b_q(i)\}]} = \frac{\frac{1}{2}\Re\left\{\boldsymbol{m}_q^H\bar{\boldsymbol{h}}_q\right\}^2}{\frac{1}{2}\Im\left\{\boldsymbol{m}_q^H\bar{\boldsymbol{h}}_q\right\}^2 + \frac{1}{2}\sum_{\substack{k=1\\k\neq q}}^{P}\left|\boldsymbol{m}_q^H\bar{\boldsymbol{h}}_k\right|^2 + \frac{1}{2}\sum_{k=P+1}^{K}\left|\boldsymbol{m}_q^H\bar{\boldsymbol{u}}_k\right|^2 + \frac{1}{2}\boldsymbol{m}_q^H\boldsymbol{R}_{\bar{n}}\boldsymbol{m}_q} \tag{29}$$

$$\mathrm{SINR}_q(\boldsymbol{\alpha}) = \frac{\frac{1}{2}\Re\left\{\boldsymbol{m}_q^H\bar{\boldsymbol{h}}_q\right\}^2}{\frac{1}{2}\Im\left\{\boldsymbol{m}_q^H\bar{\boldsymbol{h}}_q\right\}^2 + \frac{1}{2}\sum_{\substack{k=1\\k\neq q}}^{K}\left|\boldsymbol{m}_q^H\bar{\boldsymbol{h}}_k\right|^2 + \frac{1}{2}\sum_{k=P+1}^{K}\left|\boldsymbol{m}_q^H\boldsymbol{h}_k^{(2)}\right|^2 + \frac{1}{2}\boldsymbol{m}_q^H\boldsymbol{R}_{\bar{n}}\boldsymbol{m}_q} \tag{33}$$

MMSE detector in (3) can also be expressed in terms of the signal subspace components as [19]

$$\boldsymbol{m}_{q,f(q)} = \boldsymbol{U}_s \boldsymbol{\Lambda}_s^{-1} \boldsymbol{U}_s^H \boldsymbol{s}_{q,f(q)}, \quad q = 1, \ldots, P. \tag{34}$$

Corresponding to the two forms of the linear MMSE receiver (3) and (34), there are two approaches to its blind implementation [19]. In the direct-matrix-inversion (DMI) method, the autocorrelation matrix $\boldsymbol{C}_{f(q)}$ in (3) is simply replaced by the corresponding sample estimate. That is

$$\begin{aligned} \hat{\boldsymbol{C}}_{f(q)} &= \frac{1}{M} \sum_{i=1}^{M} \boldsymbol{r}_{f(q)}(2i-1) \boldsymbol{r}_{f(q)}(2i-1)^H \\ \hat{\boldsymbol{m}}_{q,f(q)} &= \hat{\boldsymbol{C}}_{f(q)}^{-1} \boldsymbol{s}_{q,f(q)} \end{aligned} \tag{35}$$

where M is the estimation sample size. In the subspace-based method, the eigencomponents $\boldsymbol{\Lambda}_s$ and $\boldsymbol{U}_s$ in (34) are replaced by the corresponding eigenvalues and eigenvectors of the sample autocorrelation matrix. That is

$$\begin{aligned} \hat{\boldsymbol{C}}_{f(q)} &= \frac{1}{M} \sum_{i=1}^{M} \boldsymbol{r}_{f(q)}(2i-1) \boldsymbol{r}_{f(q)}(2i-1)^H \\ &= \hat{\boldsymbol{U}}_s \hat{\boldsymbol{\Lambda}}_s \hat{\boldsymbol{U}}_s^H + \hat{\boldsymbol{U}}_n \hat{\boldsymbol{\Lambda}}_n \hat{\boldsymbol{U}}_n^H \\ \hat{\boldsymbol{m}}_{q,f(q)} &= \hat{\boldsymbol{U}}_s \hat{\boldsymbol{\Lambda}}_s^{-1} \hat{\boldsymbol{U}}_s^H \boldsymbol{s}_{q,f(q)}. \end{aligned} \tag{36}$$

Let $\xi \triangleq \hat{\boldsymbol{m}}_{q,f(q)}^H \boldsymbol{r}_{f(q)}(2i-1)$ be the signal at the output of the blind MMSE detector $\hat{\boldsymbol{m}}_{q,f(q)}$ obtained as in (35) or (36); relaying now takes place as follows.

DAF: When a DAF strategy is employed, at each relay $f(q) \in \mathcal{F}$ a hard symbol estimate $\tilde{b}_q(i)$ is still given by (4). Conditioned on the fading channels, we now provide closed-form expressions to approximate the asymptotic SINR and BER of both the DMI and the subspace blind MMSE detectors as function of the estimation sample size M. Let $\Delta \boldsymbol{m}_{q,f(q)} \triangleq \hat{\boldsymbol{m}}_{q,f(q)} - \boldsymbol{m}_{q,f(q)}$. We start by noticing that

$$\begin{aligned} \xi &\triangleq \hat{\boldsymbol{m}}_{q,f(q)}^H \boldsymbol{r}_{f(q)}(2i-1) \\ &= \boldsymbol{m}_{q,f(q)}^H \boldsymbol{r}_{f(q)}(2i-1) + \Delta \boldsymbol{m}_{q,f(q)}^H \boldsymbol{r}_{f(q)}(2i-1) \end{aligned} \tag{37}$$

where the first term on the right-hand side represents the output of the true detector $\boldsymbol{m}_{q,f(q)}$ in (3) or (34), while the second term represents an additional noise contribution due to the estimation error. In [21] and [20], it was shown that the error term $\Delta \boldsymbol{m}_{q,f(q)}^H \boldsymbol{r}_{f(q)}(2i-1)$ is asymptotically Gaussian distributed, whereby the conditional BER and the conditional SINR at the output of $\hat{\boldsymbol{m}}_{q,f(q)}$ can be asymptotically expressed as in (5)–(6), once the following correction term:

$$\omega(M) \triangleq \mathrm{E}\left[\Re\left\{ \Delta \boldsymbol{m}_{q,f(q)}^H \boldsymbol{r}_{f(q)}(2i-1) \right\}^2 \right] \tag{38}$$

accounting for the variance of $\Delta \boldsymbol{m}_{q,f(q)}^H \boldsymbol{r}_{f(q)}(2i-1)$ in (37) is added to the denominator of (6). The lengthy expressions of $\omega(M)$ for both the blind DMI and the blind subspace-based MMSE detectors can be found in [21].

AAF: When the AAF strategy is employed, a soft estimate of the partner's symbol is simply given by (7) once the exact MMSE filter $\boldsymbol{m}_{q,f(q)}$ is replaced by its estimate $\hat{\boldsymbol{m}}_{q,f(q)}$ in (35) or (36). Notice that the normalization factor $G_{f(q)}$ in (9) now has to be estimated from the received signals. A possible estimate is

$$\hat{G}_{f(q)} = \left(\frac{1}{M} \sum_{i=1}^{M} \left| \hat{\boldsymbol{m}}_{q,f(q)}^H \boldsymbol{r}_{f(q)}(2i-1) \right|^2 \right)^{\frac{1}{2}}. \tag{39}$$

B. Performance Analysis of DAF

In the absence of any feedback from the cooperating nodes, a robust blind implementation of the linear MMSE detector in (12) cannot be obtained. Indeed, even assuming that the true covariance matrix $\boldsymbol{C}_r$ in (14) is replaced with a sample estimate, the optimum projection direction $\bar{\boldsymbol{h}}_q$ in (13) cannot be determined without the knowledge of the interpartner link BER. Indeed, using an erroneous projection direction may lead to a significant performance loss, as shown later in Section VI. To overcome this problem, each relay has to feed back to the BS the interpartner link BER. Interestingly, this information is sufficient to evaluate not only the correct projection direction $\bar{\boldsymbol{h}}_q$ in (13) but also the exact covariance matrix $\boldsymbol{C}_r$ in (14). Thus, we have the important conclusion that, when a DAF relay strategy is employed, the exact linear MMSE detector can easily be implemented at the BS provided that each relay feeds back the interpartner link BER.

C. Performance Analysis of AAF

From (10), (22), and (25), the composite signature $\bar{\boldsymbol{h}}_q$ received at the BS can be written as $\bar{\boldsymbol{h}}_q = \boldsymbol{H}_q \boldsymbol{g}_q$, where

$$\begin{aligned} \boldsymbol{H}_q &= \left[\boldsymbol{h}_q^{(1)}, \boldsymbol{h}_1^{(2)}, \ldots, \boldsymbol{h}_{q-1}^{(2)}, \boldsymbol{h}_{q+1}^{(2)}, \ldots, \boldsymbol{h}_P^{(2)} \right] \\ \boldsymbol{g}_q &= [1, \psi_{q,1}, \ldots, \psi_{q,q-1}, \psi_{q,q+1}, \ldots, \psi_{q,P}]^T. \end{aligned} \tag{40}$$

The matrix $\boldsymbol{H}_q$ is only a function of the spreading codes and of the uplink channels of the cooperative nodes; hence, it is completely known to the BS. On the other hand, the vector $\boldsymbol{g}_q$ cannot be evaluated at the BS. Thus, under realistic assumptions, the exact linear MMSE detector cannot be constructed at the BS, but blind estimates or mismatched approximations have to be considered. In the sequel, we discuss two possible approaches to estimate this detector, corresponding to different prior knowledge about the interpartner link parameters.

First Strategy: The knowledge of $\boldsymbol{H}_q$ in (40) suggests that a blind estimate of the exact linear MMSE detector could be obtained through subspace-based techniques as in [21]. Unfortunately, since the noise vector $\bar{\boldsymbol{n}}(i)$ in (24) is colored, the signal and the noise subspaces cannot be directly identified from the covariance matrix $\boldsymbol{C}_r$ in (26). However, assuming that each cooperating terminal feeds back the power of the relayed noise, i.e., that $\boldsymbol{R}_{\bar{n}}$ in (27) is known at the BS, and, letting $\boldsymbol{R}_{\bar{n}} = \boldsymbol{V} \boldsymbol{\Sigma} \boldsymbol{V}^H$ be its eigendecomposition, the whitening transformation $\boldsymbol{W} \triangleq \boldsymbol{V} \boldsymbol{\Sigma}^{-(1/2)}$ can be obtained and the received signal can be equivalently written as $\tilde{\boldsymbol{r}}(i) = \boldsymbol{W}^H \boldsymbol{r}(i)$. Letting $\hat{\boldsymbol{C}}_{\tilde{r}} = (1/M) \sum_{i=1}^{M} \tilde{\boldsymbol{r}}(i) \tilde{\boldsymbol{r}}(i)^H$ be a sample estimate of the covariance

matrix of $\tilde{\boldsymbol{r}}(i)$, we have $\boldsymbol{C}_{\tilde{r}} = \hat{\boldsymbol{U}}_s\hat{\boldsymbol{\Lambda}}_s\hat{\boldsymbol{U}}_s^H + \hat{\boldsymbol{U}}_n\hat{\boldsymbol{\Lambda}}_n\hat{\boldsymbol{U}}_n^H$, where $\hat{\boldsymbol{\Lambda}}_s$ contains the largest K eigenvalues of $\hat{\boldsymbol{C}}_{\tilde{r}}$, $\hat{\boldsymbol{U}}_s$ contains the eigenvectors corresponding to the largest K eigenvalues in $\hat{\boldsymbol{\Lambda}}_s$, and $\hat{\boldsymbol{\Lambda}}_n$ and $\hat{\boldsymbol{U}}_n$ contain the remaining eigenvalues and eigenvectors, respectively. Letting $\tilde{\boldsymbol{H}}_q \triangleq \boldsymbol{W}^H\boldsymbol{H}_q$, the subspace-based blind estimate of $\boldsymbol{g}_q$ is given by

$$\begin{aligned}\hat{\boldsymbol{g}}_q &= \arg\min_{\|\boldsymbol{g}_q\|=1}\left\|\hat{\boldsymbol{U}}_n^H\tilde{\boldsymbol{H}}_q\boldsymbol{g}_q\right\|^2 \\ &= \arg\min_{\|\boldsymbol{g}_q\|=1}\boldsymbol{g}_q^H\underbrace{\tilde{\boldsymbol{H}}_q^H\hat{\boldsymbol{U}}_n\hat{\boldsymbol{U}}_n^H\tilde{\boldsymbol{H}}_q}_{\hat{\boldsymbol{Q}}}\boldsymbol{g}_q \\ &= \min\text{eigenvector of }\hat{\boldsymbol{Q}}\end{aligned} \tag{41}$$

whereas the corresponding subspace blind MMSE detector is

$$\hat{\boldsymbol{m}}_q = \hat{\boldsymbol{U}}_s\hat{\boldsymbol{\Lambda}}_s^{-1}\hat{\boldsymbol{U}}_s^H\tilde{\boldsymbol{H}}_q\hat{\boldsymbol{g}}_q, \quad q = 1,\ldots,P. \tag{42}$$

The estimated channel vector $\hat{\boldsymbol{g}}_q$ in (41) is determined only up to an arbitrary complex scale factor. Thus, it seems that coherent detection is not possible. Interestingly, by examining (40), the phase ambiguity can be removed by imposing that the first element of $\hat{\boldsymbol{g}}_q$ be a positive real number. Finally, similar to Section IV-A, the conditional BER and the conditional output SINR can be asymptotically expressed as in (28) and (29) once a correction term $\omega(M)$ accounting for the additional noise variance due to the estimation error is added to the denominator of (29) (the lengthy expression of $\omega(M)$ can be found in [21]).

Second Strategy: An alternative approach to approximate the exact MMSE receiver at the BS can be derived by noticing that, when the linear MMSE detector is employed at the relays, the coefficients $\{\psi_{q,k}, k \neq q, f(q)\}$ accounting for the MAI leakage are asymptotically negligible at high SNRs (see (7) and (8)). Therefore, from (7) and (25), the unknown directions $\{\bar{\boldsymbol{h}}_q, q = 1,\ldots,P\}$ and $\{\bar{\boldsymbol{u}}_q, q = P+1,\ldots,K\}$ can be approximated as

$$\begin{aligned}\bar{\boldsymbol{h}}_q &\simeq \hat{\boldsymbol{h}}_q \triangleq \boldsymbol{h}_q^{(1)} + \psi_{q,f(q)}\boldsymbol{h}_{f(q)}^{(2)}, \quad q = 1,\ldots,P \\ \bar{\boldsymbol{u}}_q &\simeq \boldsymbol{h}_q \triangleq \boldsymbol{h}_q^{(1)} + \boldsymbol{h}_q^{(2)}, \quad q = P+1,\ldots,K.\end{aligned} \tag{43}$$

In this case, assuming that each relay feeds back the coefficient $\psi_{q,f(q)}$ along with the power of the relayed noise, a mismatched approximation of the exact MMSE detector can be constructed as

$$\hat{\boldsymbol{m}}_q = \hat{\boldsymbol{C}}^{-1}\hat{\boldsymbol{h}}_q, \quad q = 1,\ldots,P \tag{44}$$

where $\hat{\boldsymbol{C}} \triangleq \sum_{k=1}^{P}\hat{\boldsymbol{h}}_k\hat{\boldsymbol{h}}_k^H + \sum_{k=P+1}^{K}\boldsymbol{h}_k\boldsymbol{h}_k^H + \boldsymbol{R}_{\tilde{n}}$. Under the Gaussian assumption of the residual MAI, the conditional SINR at the output of the linear filter (44) and the corresponding BER are still well approximated by (28) and (29).

V. Partner Selection

Let $\mathcal{T} \subseteq \{1,\ldots,K\}$ be the set of terminals that ask the BS to cooperate. The subset of terminals $\mathcal{F} \subseteq \mathcal{T}$ that can effectively take advantage from cooperation and the corresponding partner allocation should be chosen based on the average quality of all of the possible interuser links. Any partner selection mechanism should be amenable to a computationally inexpensive implementation, especially at the mobile side. Moreover, the signaling overhead should be possibly minimized; this latter point is very important in time-varying environments, where the partner assignment should be periodically updated. Based on the above considerations, we now present a simple yet effective partner selection strategy that, on the one hand, only requires a limited signaling between the active nodes and the BS, and on the other hand, takes advantage of the centralized nature of the cellular networks concentrating most of the computational processing at the BS.

At the beginning, the BS broadcasts the spreading codes of the users in the set $\mathcal{T}$. Using this information, each terminal $k \in \mathcal{T}$ monitors the average signal power received by its potential partners (for example, by using a sliding correlator or the subspace-based technique proposed in [22]) and, consequently, compiles a list of strong neighbors as follows. Let $\mathrm{NL}(k)$ be the neighbor list of the user k. A user $q \in \mathcal{T}$, with $q \neq k$, is added to $\mathrm{NL}(k)$ if and only if the average power received from q exceeds a predetermined threshold η_k; the value of η_k should be selected such that user k can reliably decode the information transmitted by any of the terminals in its neighbor list. All the neighbor lists are, then, ordered in decreasing value of the received power and sent to the BS.

Based on these lists, the BS has to decide which subset $\mathcal{F} \subseteq \mathcal{T}$ of users can benefit from cooperation and the corresponding partner assignment. In our algorithm, we suboptimally assume that partnering between any pair $(k,q) \in \mathcal{T}\times\mathcal{T}$ of users is always bidirectional and can be established only if $q \in \mathrm{NL}(k)$ and $k \in \mathrm{NL}(q)$ [5]. This latter condition, indeed, ensures that each of the two terminals reliably receives the information sent by the other. The procedure starts by assigning to each user $k \in \mathcal{T}$ a flag indicating its state: *busy* if the user already has a partner; *nonbusy* if the user does not yet have a partner but has a nonempty neighbor list; *noncooperative* if the user cannot cooperate because no partners can be found. At the beginning, the flags of the users with an empty neighbor list are set to a noncooperative state, whereas the flags of the remaining users are set to a nonbusy state. After that, the partner selection takes place as follows.

A) The nonbusy users are ordered in decreasing value of the distance from the BS and a variable CURRENT-USER is initialized to the farthest nonbusy user.
B) If the neighbors of CURRENT-USER are all in a busy or noncooperative state, then CURRENT-USER is put into a noncooperative state.
C) If there are nonbusy neighbors, they are interrogated in order to establish a cooperation. A variable CURRENT-NEIGHBOR is initialized to the first (strongest) nonbusy neighbor of CURRENT-USER.
   C-I) If CURRENT-USER $\in$ NL(CURRENT-NEIGHBOR), these two users are set as partners and put in a busy state. If this is the case, go to step D).
   C-II) If CURRENT-USER $\notin$ NL(CURRENT-NEIGHBOR), CURRENT-NEIGHBOR is

updated to the next nonbusy neighbor of CURRENT-USER, if there is any, and steps C-I) and C-II) are repeated. Otherwise, if there is no more nonbusy neighbor, CURRENT-USER is put in a noncooperative state. In this latter case, go to step D).

D) CURRENT-USER is updated to the farthest (from the BS) nonbusy user, if there is any, and steps B)–D) are repeated. The procedure ends when there is no more nonbusy user.

The proposed algorithm orders the candidate cooperative nodes according to a decreasing value of their distance from the BS and then, starting from the farthest node, tries to sequentially find the best available partner for each of them. This choice was suggested by the fact that, when path-loss effects are accounted for, terminals more distant from the BS should be privileged in the partner selection, since they can benefit from a larger energy saving with respect to closer nodes. Indeed, as shown in [5] and [6], the SNR gain provided by user cooperation can be exploited either to reduce the average transmitted power of each user $k \in \mathcal{F}$ by a factor proportional to $(d_{k,0})^{\alpha}$ or, alternatively, to extend the edge of the cell. We defer to the following performance assessment the analysis of the impact of the proposed partner allocation strategy on the overall system performance.

Finally, it is worth noticing that different policies can also be adopted to process the candidate cooperative nodes. For example, they can be processed in a pseudorandom order: in this way, on average, none of them is privileged; also, different priorities can be given to groups of users based on the quality of the requested services.

VI. Numerical Results

The analysis developed in this paper is now used to evaluate and compare the performances of the proposed cooperative protocols under different scenarios. We consider a stationary DS/CDMA network employing m-sequences as spreading codes, with a processing gain $N = 15$. The fading channels are generated considering a path loss exponent $a = 3$. We assume that average power control is present at the BS, i.e., that each terminal in the network adjusts the transmitted power such as $\mathcal{E}_k \mathrm{E}[|\alpha_{k,0}|^2] = \mathcal{E}_k/(d_{k,0})^a = \bar{\mathcal{E}}_{rx}$, for $k = 1, \ldots, K$, where $\bar{\mathcal{E}}_{rx}$ is the average power received at the BS: in this scenario, no power control is ensured at each mobile node. For the sake of simplicity, we also assume that $\mathcal{N}_0 = \mathcal{N}_1 = \cdots = \mathcal{N}_P$. The system performance is evaluated by plotting the average BERs of the cooperating terminals versus $\gamma \triangleq \bar{\mathcal{E}}_{rx}/\mathcal{N}_0$. The BERs of the nonblind receivers are obtained by numerically averaging the corresponding conditional formulas in Section III over 50 000 channel realizations. The performance of the blind detectors is assessed using the asymptotic analysis developed in Section IV.

In what follows, we first study the impact of the multiuser interference and of the partner selection on the proposed cooperative protocols when all of the system parameters are known in the system. Then, we analyze the impact of the estimation errors in the receive linear filters when some of the system parameters are unknown.

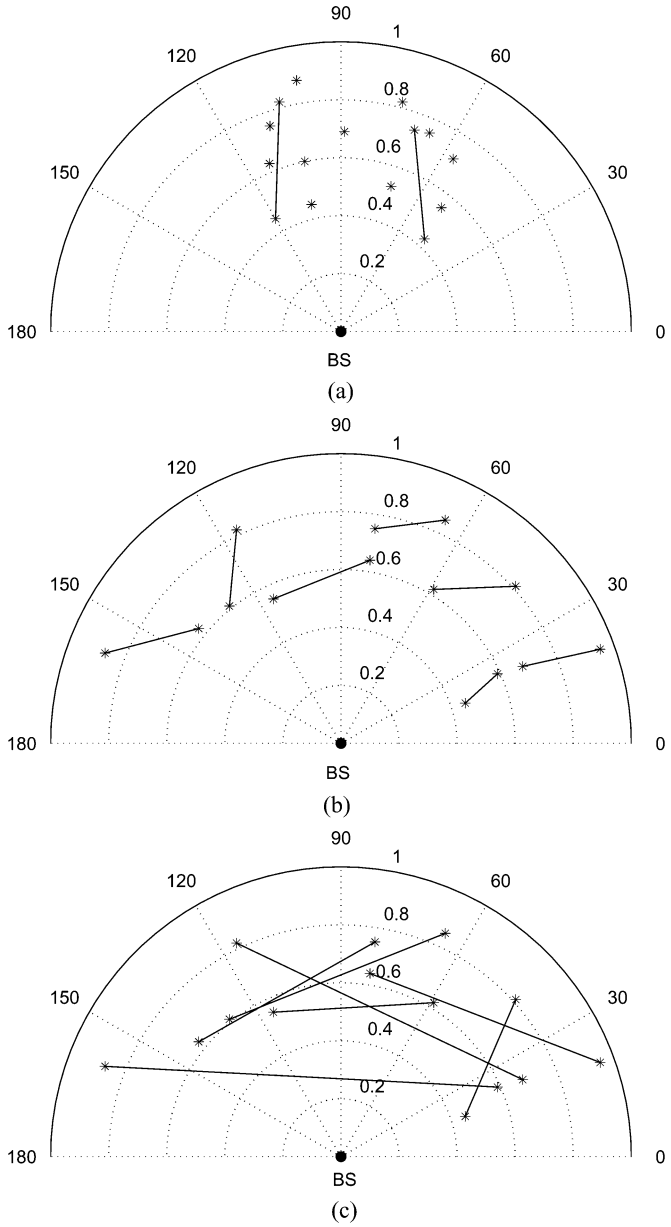

Fig. 1. Simulated stationary scenarios. The stars and the circle indicate the mobiles and the BS, respectively. In (a), 11 noncooperating users have been arbitrarily displaced around two fixed pairs of cooperating users (marked with a linking line) in order to simulate a severe near–far situation at each relay. In (b), 14 cooperating mobiles have been randomly positioned inside an angular sector of 180° and normalized internal and external radii of length 0.4 and 1, respectively; the pairs of partners have been determined by using the selection algorithm in Section V and remain fixed. In (c), the users are displaced as in (b), but the fixed pairs of partners have been randomly determined. (a) Scenario I, (b) Scenario II, and (c) Scenario III.

A. Impact of Multiuser Interference

We consider a stationary scenario where there are two fixed pairs of cooperating terminals (i.e., $P = 4$), surrounded by 11 noncooperating users (i.e., $K = 15$), as shown in Fig. 1(a) (scenario I). The nodes have been arbitrarily displaced in order to simulate a severe near–far operating condition at each relay.

In Fig. 2, we report the average BER of the cooperating users versus γ for both DAF and AAF. For the sake of comparison, we also report the average BER of the competing noncooperative (NC) network (i.e., $P = 0$ and $K = 15$), and the average BER corresponding to the ideal cooperative (IC) network

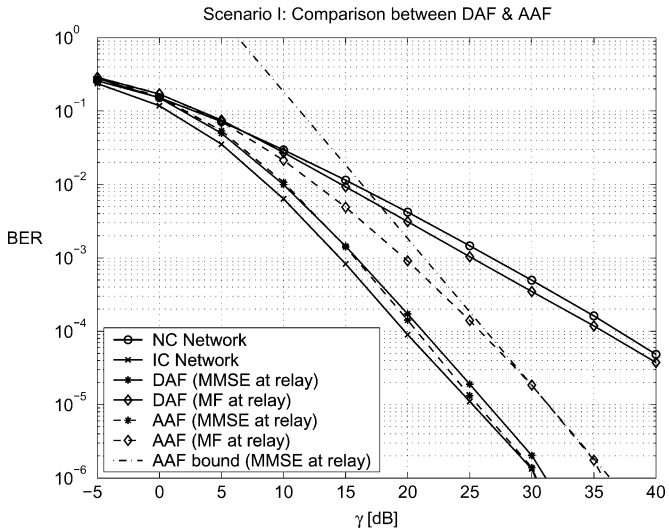

Fig. 2. BER performance of the cooperating users under ideal system assumptions. DAF and AAF are compared considering scenario I in Fig. 1(a). The exact linear MMSE detector is employed at the BS; at the relays, either the exact linear MMSE or the linear MF detector is employed. For AAF, the asymptotic upper bound in (30) is also reported.

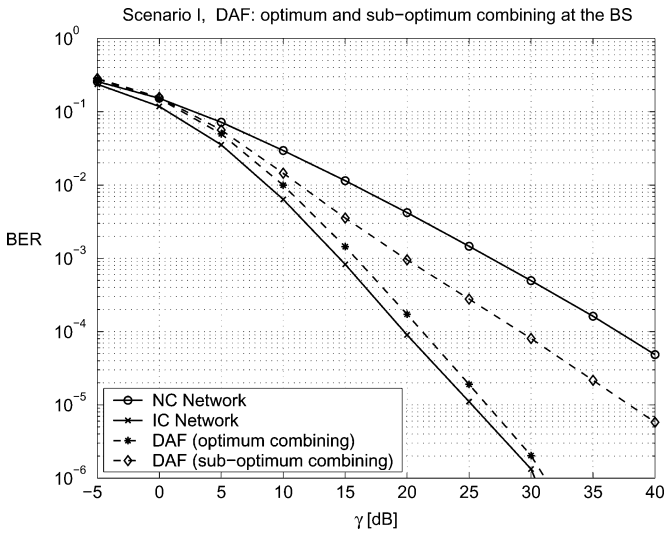

Fig. 3. BER performance of the cooperating users under ideal system assumptions. The scenario I in Fig. 1(a) and the DAF protocol are considered. At the relays, the exact linear MMSE in (3) is employed. At the BS, we consider either the exact linear MMSE in (12), which optimally combines the direct and the relayed signal replicas based on the knowledge of the interpartner link BERs, or a mismatched MMSE detector, which suboptimally assumes that the relayed symbols are error-free.

wherein partners have exact knowledge of the symbols to be relayed. When the linear MMSE detector is employed at both the relays and the BS, both DAF and AAF are immune to the multiple-access interference and provide a significant performance gain with respect to the direct transmission (15 dB at BER $= 10^{-4}$), extending previous results of [5], [6], [9], [10], and [17]. Remarkably, at high SNRs, the performance of AAF converges to the performance of the ideal cooperative network, achieving a full second-order diversity, as predicted by the upper bound in (30). If a single-user receiver is employed at the relays, both strategies experience a performance degradation. However, while DAF becomes almost ineffective due to the fact that the relayed decoded symbols are extremely unreliable (according to [17]), AAF still achieves satisfactory performance, suffering only an SNR loss due to the fact that each relay uses part of its power to forward unwanted interfering signals. Thus, in this latter case, better system performance and system robustness may be possibly traded for less computational complexity at the mobile terminals.

It is interesting to notice in Fig. 2 that, when linear multiuser detection is employed at both the relay side and the BS, DAF and AAF perform very close, suggesting that also the DAF protocol is able to achieve a quasi-full second-order diversity. A possible intuitive explanation of this result is the following. We start by noticing that, when an MMSE detector is employed at the relay side, the BER of interpartner link is noise limited [16], [18]. This means that, for large values of the channel gain $|\alpha_{q,f(q)}|$, the relayed symbols are substantially error-free, while becoming unreliable in the presence of deep fades, i.e., for small values of $|\alpha_{q,f(q)}|$. At the BS, the linear MMSE detector in (12), after interference rejection, performs a kind of modified maximal ratio combining (see also [5], [6], [9], and [17]). When the interpartner link is reliable, the two received replicas are substantially equally weighed, i.e., $\bar{\boldsymbol{h}}_q \simeq \boldsymbol{h}_q^{(1)} + \boldsymbol{h}_{f(q)}^{(2)}$; on the other hand, when the interpartner channel is in a deep fade, the relayed replica is ignored or only partially accounted for. Thus, in both cases two fading coefficients should be small for the information to be lost. Specifically, if $|\alpha_{q,f(q)}|$ is small, then $|\alpha_{q,0}|$ should also be small for the information to be lost; similarly, if $|\alpha_{q,f(q)}|$ is large, then both $|\alpha_{q,0}|$ and $|\alpha_{f(q),0}|$ should be small for the information to be lost. Notice that the key point here is that the BS has knowledge of the interpartner link BERs, which are exploited for optimal combining of the direct and relayed signal replicas. Completely different is the situation when the BS ignores the interpartner link BERs but suboptimally assumes that the relayed symbols are always corrected, as shown in Fig. 3. In this latter case, a significant performance degradation is observed, suggesting that no diversity gain is achievable.

Finally, in Fig. 4, we briefly investigate the performance of cooperation when larger constellations are employed. We only consider the AAF protocol and assume that an M-PSK constellation with $M = 16, 64$ is employed by the cooperating users; in the absence of cooperation, a $\sqrt{M}$-PSK signaling is instead adopted. As anticipated, due to the repetition nature of the protocol, the performance advantage provided by cooperation with respect to the direct transmission significantly reduces as the spectral efficiency increases, in keeping with theoretical results in [10] and [11]. In this case, more bandwidth-efficient cooperation strategies should be employed, as proposed in [10]–[14].

B. Impact of Partner Selection

To study the impact of the partner selection on the overall system performance, we consider two different partner allocations as shown in Fig. 1(b) and (c). For the sake of simplicity, we assume that users are stationary and that the pairs of cooperating terminals remain fixed over time. The allocation in Fig. 1(b) has been obtained by using the selection algorithm proposed in Section V (scenario II). To construct the neighbor lists, we have

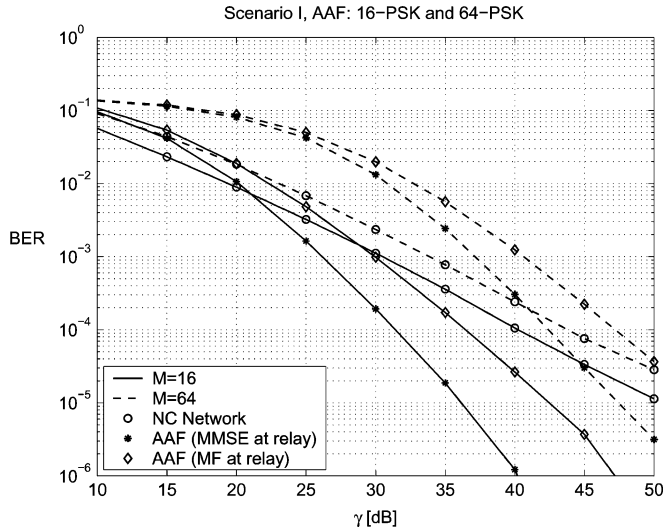

Fig. 4. BER performance of the cooperating users under ideal system assumptions. Scenario I in Fig. 1(a) and the AAF protocol are considered. The cooperating users employ an M-PSK modulation format, with $M = 16, 64$; in the absence of cooperation, a $\sqrt{M}$-PSK modulation format is instead adopted. The exact linear MMSE detector is employed at the BS; at the relays, either the exact linear MMSE or the linear MF detector is employed.

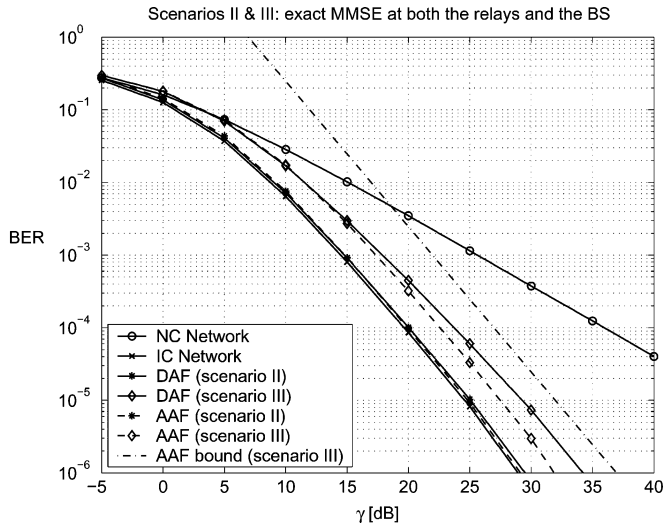

Fig. 5. BER performance of the cooperating users under ideal system assumptions. The behavior of DAF and AAF is investigated under scenarios II and III in Fig. 1(b) and (c), respectively. The exact linear MMSE detector is employed at both the relay side and the BS. For AAF, the asymptotic upper bound in (30) under scenario III is also reported.

assumed that each terminal $k \in \mathcal{T}$ selects a user $q \neq k$ as its neighbor only if the average power of the signal received by q is at least 5 dB above $\bar{\mathcal{E}}_{rx}$: in our setup, this amounts to requiring that $10 \log (d_{q,0}/d_{q,k})^a \geq 5$. The allocation in Fig. 1(c) has been obtained by randomly generating the pairs of cooperating terminals (scenario III). Notice that, while the former allocation visibly presents a more rational disposition of the cooperating pairs, for the latter, terminals transmitting from opposite sectors of the cell may try to collaborate.

Neglecting the initial signaling overhead required to allocate the partners, in Fig. 5 we compare the performance of DAF and AAF under the two scenarios described above. The linear MMSE detector is employed at both the relays and the BS. Remarkably, both DAF and AAF perform very close to the ideal case under the scenario II of Fig. 1(b), which confirms the effectiveness of the proposed partner selection algorithm, at least for this user distribution. A performance degradation is observed in the presence of a random partner allocation (scenario III): in particular, at BER$= 10^{-5}$, DAF and AAF suffer an SNR loss of about 4.5 and 2.5 dB, respectively. However, it is interesting to notice that a random partner allocation still provides a significant performance gain with respect to the direct transmission, suggesting that the use of *optimized* partner selection algorithms is not strictly necessary in order to exploit the potential benefits of cooperation. This point turns out to be very important in time-varying environments, where optimal global performance can possibly be traded for less computational expensive and/or less power and bandwidth demanding partner selection strategies. In this latter case, Fig. 5 indicates that AAF should be possibly preferred to DAF, since this protocol is less sensible to the partner choice.

We point out that studying the impact of the partner allocation on user cooperation is a challenging open problem. The analysis provided in this section only limits to repetition-based cooperation strategies applied to nonorthogonal stationary[4] DS/CDMA networks; also, only very simple partner allocation strategies have been investigated. Some intuitive indications have been drawn from our preliminary results, but much research still has to be done in this direction, especially when nonstationary scenarios are considered.

C. Impact of Estimation Errors

We now consider the effect of employing estimated linear MMSE detectors at the relay side and/or at the BS when some of the system parameters are unknown. For brevity, we only refer to scenario II in Fig. 1(b), but similar results are obtained by considering the other scenarios of Fig. 1.

In Figs. 6 and 7, we report the performance of DAF and AAF, respectively, when a subspace blind MMSE detector is employed at the relay side, while the BS receives the feedback of only one parameter related to the interpartner link (namely, the BER for DAF and the relayed noise power for AAF) from each cooperating node. For the sake of simplicity, in these plots we do not account for the extra power and bandwidth wasted by each relay terminal in the feedback channel; indeed, our main goal here is only to investigate the effectiveness and the convergence speed of the proposed linear blind multiuser detection strategies, but not to exactly quantify the performance degradation with respect to the ideal nonblind case. Interestingly, it is seen that DAF is more amenable to blind adaptive multiuser detection presenting, for increasing value of the estimation sample size M, a faster convergence to the limiting performance of the ideal scenario discussed in Fig. 5. This is

[4]When partner allocations are periodically updated in time-varying scenarios, a fair comparison between the random partner assignment and the proposed partner selection algorithm would require one to explicitly account for the additional signaling overheard generated in the network by these two allocation strategies.

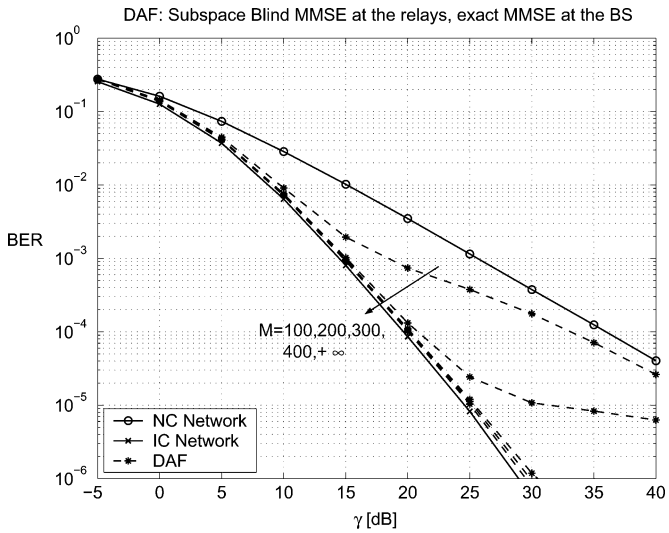

Fig. 6. BER performance of the cooperating users under realistic system assumptions when the DAF protocol is employed. The scenario in Fig. 1(b) is considered. The exact linear MMSE detector in (12) is employed at the BS; at the relays, the subspace blind MMSE detector in (36) is employed.

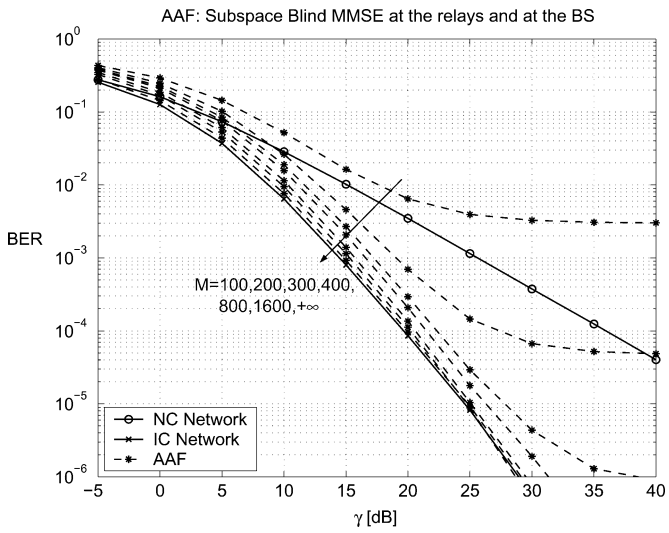

Fig. 7. BER performance of the cooperating users under realistic system assumptions, when the AAF protocol is employed. The scenario in Fig. 1(b) is considered. The subspace blind linear MMSE detectors in (36) and (42) are employed at the relays and at the BS, respectively. The same value of M is employed in both cases.

basically a consequence of the fact that, in the AAF protocol, the feedback of a single parameter from each relay is not sufficient to evaluate the exact MMSE at the BS and, thus, for small values of M, the received signal replicas cannot be effectively combined due to the presence of large estimation errors.

In Fig. 8, instead, we report the performance of AAF when a subspace blind MMSE detector is employed at the relay side but the BS receives the feedback of two parameters from each cooperating terminal: thus, the mismatched MMSE in (44) can be implemented. It is seen that, in this latter case, the convergence to the limiting performance of the ideal scenario is faster than in Fig. 7, consistent with the fact that more prior information

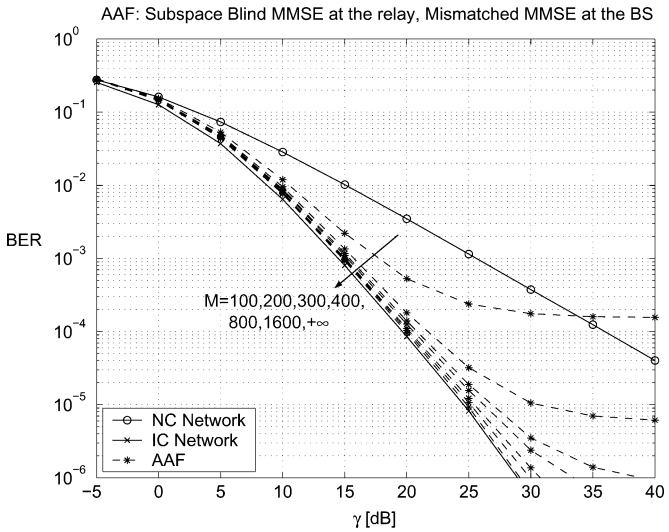

Fig. 8. BER performance of the cooperating users under realistic system assumptions, when the AAF protocol is employed. The scenario in Fig. 1(b) is considered. The subspace blind linear MMSE detector in (36) is employed at the relays, while the mismatched MMSE in (44) is employed at the BS.

about the interpartner channels is exploited at the BS. However, the price to be paid is a larger waste of bandwidth and power in the feedback channel.

VII. Conclusion

In this paper, we have investigated strategies for user cooperation in the uplink of a synchronous DS/CDMA system employing nonorthogonal spreading codes, and analyzed their performance. Two repetition-based relay schemes have been considered: DAF and AAF. We have proposed linear multiuser detection strategies at both the BS and relay terminals when the channel conditions of the systems are perfectly known; and blind multiuser detection strategies when the channel conditions are only partially known at the BS and the relays. We have provided closed-form expressions to evaluate the (asymptotic) SINR and BER for these various scenarios and have shown that AAF achieves a full second-order diversity when an MMSE detector is employed at both the relay side and the BS. We have also proposed a simple partner selection algorithm.

Using the developed analysis, several practical issues have been studied, such as the impact of the multiple-access interference and of the partner choice on the overall system performance, and the impact of imperfect knowledge of the interuser link parameters on the correct combining of the direct and relayed signal replicas. Interestingly, our results have shown that both AAF and DAF are substantially immune to the multiple-access interference when linear multiuser detection is employed, providing a significant performance gain with respect to the direct transmission. In this case, we have shown that the proposed partner allocation strategy may lead to a significant performance gain with respect to a random parter assignment, at least in stationary scenarios. Finally, it is worth noticing that, even if inferior to AAF under ideal system assumptions, DAF turns out to be more amenable to blind multiuser detection when some system parameters are unknown.

APPENDIX I
PROOF OF THE PROPOSITION 1

Proof: When the MMSE detector is employed at the relays, $\tilde{b}_q(i)$ in (7) can be expressed at high SNRs as

$$\tilde{b}_q(i) = \frac{\sqrt{\mathcal{E}_q}\alpha_{q,f(q)}b_q(i) + w_{f(q)}(2i-1)}{\sqrt{\mathcal{E}_q\left|\alpha_{q,f(q)}\right|^2 + \sigma^2_{q,f(q)}}}, \quad q = 1,\ldots,P \tag{45}$$

where $w_{f(q)}(2i-1) = (\mathcal{P}^{\perp}_{q,f(q)})^H \boldsymbol{n}_{f(q)}(2i-1) \sim \mathcal{N}(0,\sigma^2_{q,f(q)}), \sigma^2_{q,f(q)} = \mathcal{N}_{f(q)}\|\mathcal{P}^{\perp}_{q,f(q)}\|^2$ and we have exploited the fact that, at high SNRs, the MMSE detector $\boldsymbol{m}_{q,f(q)}$ in (3) converges to the zero forcing detector $\mathcal{P}^{\perp}_{q,f(q)}$ defined in (31) [16], [18].

Let us now consider the processing performed at the BS. We start by noticing that the linear MMSE receiver proposed in Section III-C exploits the signal structure in both the time domain and the space domain for MAI suppression: for this reason, in the following it is referred to as linear *space-time* MMSE detector [25]. On the other hand, it was shown in [24] and [25] that the space-time MMSE detector is always superior to the linear *diversity* MMSE detector which performs interference rejection in the time-domain only, and then exploits the spatial domain for diversity combining, i.e., $\bar{P}_q \leq \bar{P}^D_q$, where $\bar{P}^D_q$ is the average BER of the linear diversity MMSE detector.

Focusing on the linear diversity MMSE detector, after interference suppression in the time domain and using (45), the signals received at the BS during the two phases of the protocol can be asymptotically expressed as

$$y_0(2i-1) = \sqrt{\mathcal{E}_q}\alpha_{q,0}b_q(i) + w_0(2i-1), \tag{46}$$

$$\begin{aligned} y_0(2i) &= \sqrt{\mathcal{E}_{f(q)}}\alpha_{f(q),0}\tilde{b}_q(i) + w_0(2i) \\ &= \frac{\sqrt{\mathcal{E}_{f(q)}\mathcal{E}_q}\alpha_{f(q),0}\alpha_{q,f(q)}b_q(i)}{\sqrt{\mathcal{E}_q\left|\alpha_{q,f(q)}\right|^2 + \sigma^2_{q,f(q)}}} \\ &\quad + \left(\frac{w_{f(q)}(2i-1)}{\sqrt{\mathcal{E}_q\left|\alpha_{q,f(q)}\right|^2 + \sigma^2_{q,f(q)}}} + w_0(2i)\right) \end{aligned} \tag{47}$$

with $w_0(2i-1) \sim \mathcal{N}(0,\sigma^2_{q,0}), w_0(2i) \sim \mathcal{N}(0,\sigma^2_{f(q),0}), \sigma^2_{q,0} = \mathcal{N}_0\|\mathcal{P}^{\perp}_{q,0}\|^2, \sigma^2_{f(q),0} = \mathcal{N}_0\|\mathcal{P}^{\perp}_{f(q),0}\|^2$, while $\mathcal{P}^{\perp}_{q,0}$ and $\mathcal{P}^{\perp}_{f(q),0}$ are defined in (31). After optimal diversity combining of (46) and (47), the final decision statistic is given by (see also [9])

$$d = \underbrace{\sqrt{\gamma_{q,0} + \left(\frac{1}{\gamma_{f(q),0}} + \frac{1}{\gamma_{q,f(q)}} + \frac{1}{\gamma_{q,f(q)}\gamma_{f(q),0}}\right)^{-1}}}_{\sqrt{\gamma_{eq}}} \times b_q(i) + n \tag{48}$$

with $n \sim \mathcal{N}(0,1)$ and $\gamma_{q,m} \triangleq (\mathcal{E}_q|\alpha_{q,m}|^2)/(\sigma^2_{q,m})$. Letting $\bar{\gamma}_{q,m} \triangleq \mathrm{E}[\gamma_{q,m}]$, we now have (49) as shown at the bottom of the page, where we have used the fact that $Q(x) \leq (1/2)\exp\{-(x^2/2)\}$ for $x \in [0,+\infty)$, while the statistical expectation is intended over $\gamma_{q,f(q)}, \gamma_{q,0}$ and $\gamma_{f(q),0}$. Under Rayleigh fading, the term A in (49) is easily upper bounded as follows:

$$\begin{aligned} A &= \frac{1}{2}\int_0^{+\infty} \frac{1}{\bar{\gamma}_{q,0}} \exp\left\{-\frac{x}{\bar{\gamma}_{q,0}}\right\} \exp\left\{-\frac{x}{2}\right\} dx \\ &= \frac{1}{\bar{\gamma}_{q,0}+2} \leq \frac{1}{\bar{\gamma}_{q,0}}. \end{aligned} \tag{50}$$

As to B, upon defining for notational simplicity $\lambda_x = \bar{\gamma}_{q,f(q)}$ and $\lambda_y = \bar{\gamma}_{f(q),0}$, for large SNRs (i.e., $\lambda_x, \lambda_y \to +\infty$), we now prove the result shown in (51)–(53) at the bottom of the page.

$$\bar{P}_q \leq \bar{P}^D_q = \mathrm{E}\left[Q\left(\sqrt{\gamma_{eq}}\right)\right] \leq \underbrace{\frac{1}{2}\mathrm{E}\left[\exp\left\{-\frac{\gamma_{q,0}}{2}\right\}\right]}_{A} \underbrace{\mathrm{E}\left[\exp\left\{-\frac{1}{2}\left(\frac{1}{\gamma_{f(q),0}} + \frac{1}{\gamma_{q,f(q)}} + \frac{1}{\gamma_{q,f(q)}\gamma_{f(q),0}}\right)^{-1}\right\}\right]}_{B} \tag{49}$$

$$B = \underbrace{\int_0^{+\infty} \exp\left\{-\frac{y}{\lambda_y}\right\}\frac{dy}{\lambda_y}\int_0^{\lambda_x} \exp\left\{-\frac{1}{2}\left(\frac{xy}{x+y+1}\right)\right\}\exp\left\{-\frac{x}{\lambda_x}\right\}\frac{dx}{\lambda_x}}_{B_1} \tag{51}$$

$$+ \underbrace{\int_0^{+\infty} \exp\left\{-\frac{y}{\lambda_y}\right\}\frac{dy}{\lambda_y}\int_{\lambda_x}^{+\infty} \exp\left\{-\frac{1}{2}\left(\frac{xy}{x+y+1}\right)\right\}\exp\left\{-\frac{x}{\lambda_x}\right\}\frac{dx}{\lambda_x}}_{B_2} \tag{52}$$

$$\leq 4\left(\frac{1}{\lambda_x} + \frac{1}{\lambda_y}\right) + \mathcal{O}\left(\frac{1}{\lambda_x}\right) + \mathcal{O}\left(\frac{1}{\lambda_y}\right). \tag{53}$$

We start by evaluating the term B_1 in (51). The inner integral can be upper bounded as follows:

$$\begin{aligned}
&\int_0^{\lambda_x} \exp\left\{-\frac{1}{2}\left(\frac{xy}{x+y+1}\right)\right\}\exp\left\{-\frac{x}{\lambda_x}\right\}\frac{dx}{\lambda_x} \\
&\quad\le \int_0^{\lambda_x} \exp\left\{-x\left(\frac{y}{2(\lambda_x+y+1)}+\frac{1}{\lambda_x}\right)\right\}\frac{dx}{\lambda_x} \\
&\quad= \frac{1}{\frac{y\lambda_x}{2(\lambda_x+y+1)}+1} \\
&\qquad\times\left[1-\exp\left\{-\lambda_x\left(\frac{y}{2(\lambda_x+y+1)}+\frac{1}{\lambda_x}\right)\right\}\right] \\
&\quad\le \frac{2y+2(\lambda_x+1)}{y(\lambda_x+1)+2(\lambda_x+1)} \qquad (54)
\end{aligned}$$

where in the first inequality we have used the fact that $(xy)/(x+y+1) \ge (xy)/(\lambda_x+y+1)$ for $x \in [0,\lambda_x]$. Averaging (54) over y, we now have

$$\begin{aligned}
B_1 &\le \int_0^{+\infty} \frac{2y+2(\lambda_x+1)}{y(\lambda_x+1)+2(\lambda_x+1)}\exp\left\{-\frac{y}{\lambda_y}\right\}\frac{dy}{\lambda_y} \\
&= \frac{2}{\lambda_y(\lambda_x+1)}\left[2\exp\left\{\frac{2}{\lambda_y}\right\}Ei\left(-\frac{2}{\lambda_y}\right)+\lambda_y\right] \\
&\quad -\frac{2}{\lambda_y}\exp\left\{\frac{2}{\lambda_y}\right\}Ei\left(-\frac{2}{\lambda_y}\right) \qquad (55) \\
&= \frac{2}{\lambda_x+1}-\frac{2}{\lambda_y}\exp\left\{\frac{2}{\lambda_y}\right\}Ei\left(-\frac{2}{\lambda_y}\right)\left[\frac{\lambda_x-1}{\lambda_x+1}\right] \qquad (56)
\end{aligned}$$

where $Ei(\cdot)$ is the exponential integral function, and in (55) we used the result (see [26, para. 3.353])

$$\begin{aligned}
&\int_0^{+\infty}\frac{x^n\exp\{-\mu x\}}{x+\beta}dx \\
&\quad= (-1)^{n-1}\beta^n\exp\{\beta\mu\}Ei(-\beta\mu) \\
&\qquad+\sum_{k=1}^{n}(k-1)!(-\beta)^{n-k}\mu^{-k}. \qquad (57)
\end{aligned}$$

Since $Ei(-z) = C+\ln(z)+\sum_{k=1}^{+\infty}((-1)^k z^k)/(k\cdot k!)$ for $z>0$ (see [26, para. 8.214]), $C\approx 0.577$ being Euler's constant, for large values of λ_x and λ_y, we have

$$\begin{aligned}
B_1 &\le \int_0^{+\infty}\frac{2y+2(\lambda_x+1)}{y(\lambda_x+1)+2(\lambda_x+1)} \\
&\quad\times\exp\left\{-\frac{y}{\lambda_y}\right\}\frac{dy}{\lambda_y} \to \frac{2}{\lambda_x+1}+\frac{2(1-C)}{\lambda_y} \\
&\quad+\mathcal{O}\left(\frac{2}{\lambda_y}\right) \le \frac{2}{\lambda_x}+\frac{2}{\lambda_y}+\mathcal{O}\left(\frac{2}{\lambda_y}\right). \qquad (58)
\end{aligned}$$

We now evaluate the term B_2 in (52). The inner integral can be upper bounded as follows:

$$\begin{aligned}
&\int_{\lambda_x}^{+\infty}\exp\left\{-\frac{1}{2}\left(\frac{xy}{x+y+1}\right)\right\}\exp\left\{-\frac{x}{\lambda_x}\right\}\frac{dx}{\lambda_x} \\
&\qquad\le \exp\left\{-\frac{1}{2}\left(\frac{\lambda_x y}{\lambda_x+y+1}\right)\right\} \qquad (59)
\end{aligned}$$

where we have exploited the fact that $(xy)/(x+y+1) \ge (\lambda_x y)/(\lambda_x+y+1)$ for $x\in[\lambda_x,+\infty]$. Averaging (59) over y, we now have

$$\begin{aligned}
B_2 &\le \int_0^{+\infty}\exp\left\{-\frac{1}{2}\left(\frac{\lambda_x y}{\lambda_x+y+1}\right)\right\}\exp\left\{-\frac{y}{\lambda_y}\right\}\frac{dy}{\lambda_y} \\
&= \underbrace{\int_0^{\lambda_y}\exp\left\{-\frac{1}{2}\left(\frac{\lambda_x y}{\lambda_x+y+1}\right)\right\}\exp\left\{-\frac{y}{\lambda_y}\right\}\frac{dy}{\lambda_y}}_{B_2^{(I)}} \\
&\quad+\underbrace{\int_{\lambda_y}^{+\infty}\exp\left\{-\frac{1}{2}\left(\frac{\lambda_x y}{\lambda_x+y+1}\right)\right\}\exp\left\{-\frac{y}{\lambda_y}\right\}\frac{dy}{\lambda_y}}_{B_2^{(II)}} \\
&\le \frac{2}{\lambda_x}+\frac{2}{\lambda_y}+\exp\left\{-\frac{1}{2}\left(\frac{\lambda_x\lambda_y}{\lambda_x+\lambda_y+1}\right)\right\}. \qquad (60)
\end{aligned}$$

In the last inequality, we have exploited the fact that:

$$\begin{aligned}
B_2^{(I)} &\le \int_0^{\lambda_y}\exp\left\{-\frac{\lambda_x y}{2(\lambda_x+\lambda_y+1)}\right\} \\
&\quad\times\exp\left\{-\frac{y}{\lambda_y}\right\}\frac{dy}{\lambda_y} = \frac{1}{\frac{\lambda_x\lambda_y}{2(\lambda_x+\lambda_y+1)}+1} \\
&\quad\times\left[1-\exp\left\{-\left(\frac{\lambda_x\lambda_y}{2(\lambda_x+\lambda_y+1)}+1\right)\right\}\right] \\
&\le \frac{2(\lambda_x+\lambda_y+1)}{\lambda_x\lambda_y+2\lambda_x+2\lambda_y+2} \\
&\le \frac{2}{\lambda_x+1}+\frac{2}{\lambda_y+1} \le \frac{2}{\lambda_x}+\frac{2}{\lambda_y} \qquad (61) \\
B_2^{(II)} &\le \exp\left\{-\frac{1}{2}\left(\frac{\lambda_x\lambda_y}{\lambda_x+\lambda_y+1}\right)\right\}\int_{\lambda_y}^{+\infty}\exp\left\{-\frac{y}{\lambda_y}\right\}\frac{dy}{\lambda_y} \\
&\le \exp\left\{-\frac{\lambda_x\lambda_y}{2(\lambda_x+\lambda_y+1)}\right\}. \qquad (62)
\end{aligned}$$

From (58) and (60), for large SNRs, we obtain

$$\begin{aligned}
&\mathrm{E}\left[\exp\left\{-\frac{1}{2}\left(\frac{1}{\gamma_{f(q),0}}+\frac{1}{\gamma_{q,f(q)}}+\frac{1}{\gamma_{q,f(q)}\gamma_{f(q),0}}\right)^{-1}\right\}\right] \\
&\qquad\le 4\left(\frac{1}{\lambda_x}+\frac{1}{\lambda_y}\right)+\mathcal{O}\left(\frac{2}{\lambda_y}\right). \qquad (63)
\end{aligned}$$

Repeating the same derivation inverting the roles of x and y, we can also obtain

$$\begin{aligned}
&\mathrm{E}\left[\exp\left\{-\frac{1}{2}\left(\frac{1}{\gamma_{f(q),0}}+\frac{1}{\gamma_{q,f(q)}}+\frac{1}{\gamma_{q,f(q)}\gamma_{f(q),0}}\right)^{-1}\right\}\right] \\
&\qquad\le 4\left(\frac{1}{\lambda_x}+\frac{1}{\lambda_y}\right)+\mathcal{O}\left(\frac{2}{\lambda_x}\right). \qquad (64)
\end{aligned}$$

Thus, (53) easily follows from (63) and (64). Finally, (30) is obtained from (49), (50), and (53). ■

REFERENCES

[1] J. G. Proakis, *Digital Communications*, 4th ed. New York: McGraw-Hill, 2001.

[2] L. Zheng and D. N. C. Tse, "Diversity and multiplexing: A fundamental tradeoff in multiple-antenna channels," *IEEE Trans. Inf. Theory*, vol. 49, no. 5, pp. 1073–1096, May 2003.

[3] D. Gesbert, M. Shafi, D. Shiu, P. J. Smith, and A. Naguib, "From theory to practice: An overview of MIMO space-time coded wireless systems," *IEEE J. Sel. Areas Commun.*, vol. 21, no. 3, pp. 281–302, Apr. 2003.

[4] G. J. Foschini, D. Chizhik, M. J. Gans, C. Papadias, and R. A. Valenzuela, "Analysis and performance of some basic space-time architectures," *IEEE J. Sel. Areas Commun.*, vol. 21, no. 3, pp. 303–320, Apr. 2003.

[5] A. Sendonaris, E. Erkip, and B. Aazhang, "User cooperation diversity—Part I: System description," *IEEE Trans. Commun.*, vol. 51, no. 11, pp. 1927–1938, Nov. 2003.

[6] A. Sendonaris, E. Erkip, and B. Aazhang, "User cooperation diversity—Part II: Implementation aspects and performance analysis," *IEEE Trans. Commun.*, vol. 51, no. 11, pp. 1939–1948, Nov. 2003.

[7] M. Dohler, E. Lenfranc, and H. Aghvami, "Space-time block codes for virtual arrays," in *Proc. 2002 IEEE PIMRC*, Sept. 2002, vol. 1, pp. 414–417.

[8] M. Dohler, F. Said, and H. Aghvami, "High order space-time block codes for virtual antenna arrays," in *Proc. 2003 Int. Conf. Telecommunications*, Feb. 2003, vol. 1, pp. 198–203.

[9] J. N. Laneman and G. W. Wornell, "Energy-efficient antenna sharing and relaying for wireless networks," in *Proc. 2000 IEEE Wireless Communications Networking Conf. (WCNC)*, Sep. 2000, vol. 1, pp. 7–12.

[10] J. N. Laneman, D. N. C. Tse, and G. W. Wornell, "Cooperative diversity in wireless networks: Efficient protocols and outage behavior," *IEEE Trans. Inf. Theory*, vol. 50, pp. 389–400, Dec. 2004.

[11] J. N. Laneman and G. W. Wornell, "Distributed space-time coded protocols for exploiting cooperative diversity in wireless networks," *IEEE Trans. Inf. Theory*, vol. 49, pp. 3062–3080, Oct. 2003.

[12] T. E. Hunter and A. Nosratinia, "Cooperation diversity through coding," in *Proc. 2002 IEEE Int. Symp. Inf. Theory (ISIT)*, Lausanne, Switzerland, p. 220.

[13] A. Stefanov and E. Erkip, "Cooperative coding for wireless networks," *IEEE Trans. Commun.*, vol. 52, no. 9, pp. 1470–1476, Sep. 2004.

[14] M. Janani, A. Hedayat, T. E. Hunter, and A. Nosratinia, "Coded cooperation in wireless communications: Space-time transmission and iterative decoding," *IEEE Trans. Signal Process.*, vol. 52, no. 2, pp. 362–371, Feb. 2004.

[15] A. Nosratinia, T. E. Hunter, and A. Hedayat, "Cooperative communication in wireless networks," *IEEE Commun. Mag.*, vol. 42, no. 10, pp. 74–80, Oct. 2004.

[16] S. Verdù, *Multiuser Detection*. Cambridge, U.K.: Cambridge Univ., 1998.

[17] Y. Cao and B. Vojcic, "MMSE multiuser detection for cooperative diversity CDMA systems," in *Proc. 2004 IEEE WCNC*, Atlanta, GA, pp. 42–47.

[18] H.V. Poor and S. Verdú, "Probability of error in MMSE multiuser detection," *IEEE Trans. Inf. Theory*, vol. 43, pp. 858–871, Mar. 1997.

[19] X. Wang and H.V. Poor, "Blind multiuser detection: A subspace approach," *IEEE Trans. Inf. Theory*, vol. 44, pp. 677–690, Mar. 1998.

[20] A. Høst-Madsen and X. Wang, "Performance of blind and group-blind multiuser detectors," *IEEE Trans. Inf. Theory*, vol. 48, pp. 1849–1872, Jul. 2002.

[21] A. Høst-Madsen, X. Wang, and S. Bahng, "Asymptotic analysis of blind multiuser detection with blind channel estimation," *IEEE Trans. Signal Process.*, vol. 52, no. 6, pp. 1722–1738, Jun. 2004.

[22] S. E. Bensley and B. Aazhang, "Subspace-based channel estimation for code division multiple access communication systems," *IEEE Trans. Commun.*, vol. 44, pp. 1009–1020, Aug. 1996.

[23] J. Cheng and N. C. Beaulieu, "Accurate DS-CDMA bit-error-rate probability calculation in Rayleigh fading," *IEEE Trans. Wireless Commun.*, vol. 1, pp. 3–15, Jan. 2002.

[24] S. Y. Miller and S. C. Schwartz, "Integrated spatial-temporal detectors for asynchronous Gaussian multiple-access channels," *IEEE Trans. Commun.*, vol. 43, pp. 396–411, Feb./Mar./Apr. 2004.

[25] D. Reynolds, X. Wang, and H. V. Poor, "Blind adaptive space-time multiuser detection with multiple transmitter and receiver antennas," *IEEE Trans. Signal Process.*, vol. 50, no. 6, pp. 1261–1276, Jun. 2002.

[26] I. S. Gradshteyn and I. M. Ryzhik, *Table of Integrals, Series, and Products (Corrected and Enlarged Edition)*. New York: Academic, 1980.

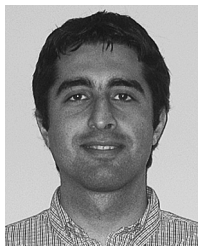

Luca Venturino (S'03–M'06) was born in Cassino, Italy, on August 26, 1979. He received the Dr.Eng. degree in telecommunication engineering and the Ph.D. degree in electrical engineering from the University of Cassino in 2002 and 2006, respectively.

In 1999 and 2000, he was a summer student at the Fermi National Laboratory of Chicago, Chicago, IL, as a summer student. From September 2001 through February 2002, he was with the University of Bath, Bath, U.K., under the Socrates/Erasmus exchange program. In 2004, he was a Visiting Scholar with the Department of Electrical Engineering of the Columbia University, New York. In 2006, he spent three months as a visiting Researcher at the NEC Laboratories America, Princeton, NJ. Currently, he is an Assistant Professor at the University of Cassino, Italy. His research interests concern wireless multiuser communication systems in CDMA applications, MIMO systems with space-time coding, and signal detection for radar systems.

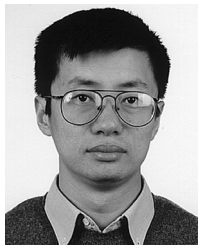

Xiaodong Wang (S'98–M'98–SM'04) received the B.S. degree from Shanghai Jiao Tong University, Shanghai, China, the M.S. degree from Purdue University, West Lafayette, IN, and the Ph.D. degree from Princeton University, Princeton, NJ, all in electrical engineering.

From July 1998 to December 2001, he was on the Faculty of the Department of Electrical Engineering, Texas A&M University, College Station. Since January 2002, he has been with the Department of Electrical Engineering, Columbia University, New York. His research interests fall in the general areas of computing, signal processing, and communications, and he has published extensively in these areas. Among his publications is *Wireless Communication Systems: Advanced Techniques for Signal Reception* (Englewood Cliffs, NJ: Prentice-Hall, 2003). His current research interests include wireless communications, statistical signal processing, and genomic signal processing.

Dr. Wang received the 1999 NSF CAREER Award and the 2001 IEEE Communications Society and Information Theory Society Joint Paper Award. He currently is an Associate Editor for the IEEE TRANSACTIONS ON COMMUNICATIONS, IEEE TRANSACTIONS ON WIRELESS COMMUNICATIONS, IEEE TRANSACTIONS ON SIGNAL PROCESSING, and IEEE TRANSACTIONS ON INFORMATION THEORY.

Marco Lops (M'96–SM'01) was born in Naples, Italy, on March 16, 1961. He received the Dr.Eng. and Ph.D. degrees in electronic engineering from the University of Naples in 1986 and 1992, respectively.

From 1986 to 1987, he was in Selenia, Rome, Italy, as an Engineer with the Air Traffic Control Systems Group. From 1991 to 2000, he was an Associate Professor of radar theory and digital transmission theory at the University of Naples. Since March 2000, he has been a full Professor at the University of Cassino, engaged in research in the field of statistical signal processing, with emphasis on radar processing and spread-spectrum multiuser communications. He also held teaching positions with the University of Lecce. During 1991, 1998, and 2000, he was on sabbatical leaves with the University of Connecticut, Rice University, and Princeton University, respectively.